European Journal of Pharmaceutics and Biopharmaceutics 139 (2019) 101–114

Contents lists available at ScienceDirect

European Journal of Pharmaceutics and Biopharmaceutics

journal homepage: www.elsevier.com/locate/ejpb

Review article

Biorelevant intrinsic dissolution profiling in early drug development: Fundamental, methodological, and industrial aspects

Christel A.S. Bergström[a,*], Karl Box[b], René Holm[c], Wayne Matthews[d], Mark McAllister[e], Anette Müllertz[f], Thomas Rades[f], Kerstin J. Schäfer[g], Alexandra Teleki[a]

[a] Department of Pharmacy, Uppsala University, Uppsala Biomedical Center, P.O. Box 580, SE-75123 Uppsala, Sweden
[b] pION Inc, Forest Row Business Park, Forest Row, East Sussex RH18 5DW, UK
[c] Drug Product Development, Janssen R&D, Johnson & Johnson, Turnhoutseweg 30, 2340 Beerse, Belgium
[d] Department of Product Development, GlaxoSmith Kline Medicines Research Centre, 2G118, Gunnels Wood Road, Stevenage, Herts, UK
[e] Drug Product Design, Pharmaceutical Sciences, Pfizer Ltd., Sandwich CT13 9NJ, Kent, UK
[f] Department of Pharmacy, Faculty of Health and Medical Sciences, University of Copenhagen, Universitetsparken 2, DK-2100 Copenhagen, Denmark
[g] Pharmaceutical Development, Boehringer Ingelheim Pharma GmbH & Co KG, Birkendorfer strasse 65, 88397 Biberach an der Riss, Germany

ABSTRACT

Intrinsic dissolution rate (IDR) is the surface specific dissolution rate of a drug. In early drug development, this property (among other parameters) is measured in order to compare different polymorphs and salt forms, guide formulation decisions, and to provide a quality marker of the active pharmaceutical ingredient (API) during production. In this review, an update on different methods and small-scale techniques that have recently evolved for determination of IDR is provided. The importance of biorelevant media and the hydrodynamic conditions of dissolution are also discussed. Different preparation techniques for samples are presented with a focus on disc, particle- and crystal-based methods. A number of small-scale techniques are then described in detail, and their applicability domains are identified. Finally, an updated industrial perspective is provided about IDR's place in the early drug development process.

1. Introduction: basic concepts and the importance of dissolution profiling

The Biopharmaceutics Classification System (BCS) was designed based on the recognition of the importance of both solubility and permeability on the fraction absorbed of a drug [1]. This system was developed for regulatory purposes with the objective of identifying compounds for which *in vitro*-based biowaivers could be obtained without conducting clinical bioequivalent studies. The BCS sorts compounds into four classes based on cut-off values for high and low solubility (complete dose dissolved in 250 mL of water at pH 1–6.8) and permeability (> 85% of the dissolved dose being absorbed). In this system, Class 2 and 4 compounds are those with low solubility. Class 2 compounds have too low a solubility to allow complete absorption, whereas Class 4 compounds have both low solubility and low permeability. A large number of drug discovery and development compounds have been identified as being BCS Class 2, with estimates ranging from 50 to 60% of such compounds up to as high as 90% [2,3].

Important limitations of the BCS as it currently stands have also been identified. These limitations include (i) over-emphasis on dissolution in the gastric compartment for weak acids with a pKa < 5, (ii) the higher buffer capacity of common buffers and media used for dissolution profiling than buffering capacities observed *in vivo* [4–6] and (iii) the lack of bile components (bile salts, phospholipids, lipids, cholesterol) in defined BCS dissolution media [7–11]. The first limitation (overemphasis on the gastric compartment) means that compounds with limited dissolution in the stomach, but complete dissolution in the small intestine (where the majority of the absorption occurs), are

Abbreviations: AFM, atomic force microscopy; API, active pharmaceutical ingredient; BCDI, bragg coherent diffraction imaging; BCS, biopharmaceutics classification system; CFD, computational fluid dynamics; CMC, critical micellar concentration; CMOS, complementary metal-oxide-semiconductor; C_s, saturated concentration; DCS, developability classification system; DIDR, disc intrinsic dissolution rate; DSC, differential scanning calorimetry; FaSSIF, fasted state simulated intestinal fluid; FeSSIF, fed state simulated intestinal fluid; FL, fluorescence; HPLC, high-performance liquid chromatography; HPMC, hydoxypropylmethylcellulose; IDR, intrinsic dissolution rate; MEC, molar extinction coefficient; MS, mass spectroscopy; NIR, near infrared; P80, polysorbate 80; Pe, Peclet number; PIDR, powder intrinsic dissolution rate; PVP, polyvinylpyrrolidone; rDCS, refined DCS; RPM, revolutions per minute; S_{app}, apparent solubility; SDI, surface dissolution imaging; SDS, sodium dodecyl sulfate; SEM, scanning electron microscopy; SIDR, suspension intrinsic dissolution rate; SSA, specific surface area; TEM, transmission electron microscopy; TPGS, D-α-tocopherol polyethylene glycol 1000 succinate; UPLC, ultra-performance liquid chromatography; USP, US pharmacopeia; UV-VIS, Ultraviolet-visible; XPS, X-ray photoelectron spectroscopy; XRD, X-ray diffraction

* Corresponding author at: Department of Pharmacy, Uppsala University, Uppsala Biomedical Center, Box 580, SE-751 23 Uppsala, Sweden.
E-mail address: christel.bergstrom@farmaci.uu.se (C.A.S. Bergström).

https://doi.org/10.1016/j.ejpb.2019.03.011
Received 14 October 2018; Received in revised form 7 February 2019; Accepted 8 March 2019
Available online 09 March 2019
0939-6411/

defined as low solubility compounds, and are therefore sorted as compounds limited in their absorption by their solubility [12,13]. The second limitation (a mismatch between *in vitro* and *in vivo* buffer capacity) means that the potential for self-buffering effects at the surface of the non-dissolved active pharmaceutical ingredient (API) are underestimated, which in turn results in a greater dissolution rate measured *in vitro* than happens *in vivo*. The effect of buffer capacity can be calculated if pKa and the intrinsic solubility of the drug is known. The third limitation (lack of bile components) means that the solubilization of highly lipophilic compounds in the bile components of the intestinal fluid is underestimated. Commonly, this effect is expected to be significant for compounds with a logarithmic partition coefficient between octanol and water (log P > 3) [14].

To address those shortcomings and guide relevant formulation strategies based on more accurate measurements of dissolution (rate) and solubility (extent) of discovery compounds, the Developability Classification System (DCS) has been proposed [15,16]. The original DCS was designed to more rigorously determine which factor is rate-limiting for drug absorption, not as a regulatory tool. Compared to the BCS, the DCS is based on more realistic GI tract volumes to provide a sink (500 mL total volume of fluid in the fasted state) as well as the compensatory nature of permeability on low solubility. The DCS was recently refined (rDCS) to enable more custom-based experiments for exploring dissolution, solubility, supersaturation, precipitation and permeation, and through this approach, to more easily compare compounds and formulations with each other [15].

There has been a longstanding discussion on which particular medium or method one should use to achieve biorelevant dissolution and produce biorelevant solubility data of compounds, and a number of different simulated intestinal fluids have been proposed [17–21]. In addition to solubilization, colloidal structures such as micelles and vesicles formed by the bile components may influence the dissolution rate in a more complex manner for compounds that are extensively solubilized. The relationship between solubility, diffusion, and dissolution rate is described by the Noyes-Whitney equation [22]:

$$\frac{dC}{dt} = \frac{D}{h}A(C_S - C_t) \quad (1)$$

where dC/dt is the change in concentration over time (i.e. dissolution rate), D is the diffusion coefficient (cm^2/s), h is the thickness of the diffusion layer (cm), A is the surface area (cm^2), C_s is the saturated concentration (i.e. the thermodynamic solubility), and C_t is the concentration of the dissolved compound in the bulk at time t. Concentration is often reported as μg/mL. From the equation, it is clear that the dissolution rate should increase with increased solubility and increased surface area. Common formulation tools used to improve a compound's dissolution rate include the addition of cosolvents and surfactants (to increase solubility) and the reduction of particle size (micronization or nanonization, to increase the surface area of the dissolving material) [23].

As shown by the Noyes-Whitney equation, the dissolution rate is further dependent on the diffusion of molecules away from the surface-solvent interface. The effective diffusion (D_{eff}) for extensively solubilized drugs is a result of the molecular and the micelle diffusion, as described by the following equation:

$$D_{eff} = D_u f_u + D_m f_m \quad (2)$$

where D_u and D_m are the average diffusion coefficients of the unbound drug and the micelle, respectively, and f_u and f_m are the fraction of drug being unbound and bound to micelles, respectively [24,25]. The diffusion coefficient (D; m/s) can be calculated by the Stokes-Einstein equation:

$$D = \frac{kT}{6\pi\eta r} \quad (3)$$

where k is the Boltzmann constant (J/K), T is the temperature (K), η is the viscosity of the solvent ($N \times s/m^2$), and r is the radius (m) of the diffusant. Theoretical calculations of the diffusion coefficient have been further developed by, among others, the Wilke-Chang, Scheibel, Lusis-Ratcliff, and Hayduk-Laudie correlations [26–29]. Diffusion coefficients can also be determined experimentally, most commonly by pulsed-gradient spin-echo NMR [30] or Taylor dispersion analysis using capillary electrophoresis instrumentation [31–33].

Methods have been developed to assess the dissolution rate of the drug under different conditions, such as at gastrointestinal pH and bile content levels. Formulation scientists also use dissolution profiling to choose suitable excipients of the formulation and select the dosage form with the most appropriate and reproducible release profile [34]. Like solubility, dissolution rate is typically reported as the amount/volume (e.g., μg/mL) that is dissolved per a specified time unit. To compare different formulations and dosage forms, dissolution rate is also commonly presented as the percentage of drug dissolved (i.e. of the total amount of drug added to the dissolution vial) per time unit. For a dosage form of a BCS Class 1 compound (i.e. high solubility, high permeability) to be regarded as an immediate release formulation, 80% of the maximum dose should dissolve in 500 mL of dissolution medium within 30 min [35], as assessed by a USP 1 (Basket) or USP 2 (Paddle) dissolution apparatus.

A more standardized measurement of dissolution is the intrinsic dissolution rate (IDR, $\mu g/min/cm^2$), which is the dissolution rate adjusted for the surface area of the compound. IDR is an intrinsic property that is suitable to assess in a number of situations, for example during salt selections, when exploring the impact of polymorph changes on dissolution, and when investigating to what extent micronization may overcome hurdles such as dissolution-limited absorption. IDR is typically measured using a rotating disc of compacted powder, with a defined surface area, in contact with the dissolution medium [36,37]. However, assays using powder dispersed into the medium can determine IDR much more rapidly. The significantly greater surface area in contact with the dissolution medium can reduce the time needed for measurement from hours to minutes for poorly water-soluble compounds. In the following sections, the different methods currently used to determine IDR will be described, followed by an update of various small-scale technologies useful for IDR measurements. In the final section, an industrial view of the benefits of determining IDR as a complement to the more traditional dissolution profiling will be provided.

2. Methods

This review is based on one of the tasks in the IMI project OrBiTo. The full OrBiTo project has had the goal to enhance our understanding of how orally administered drugs are taken up by the gastrointestinal tract into the systemic circulation, and furthermore, to apply this knowledge to develop new experimental and computational models that will better predict performance of such drugs in patients. In the work with physicochemical characterization of drugs, particular efforts were directed towards exploration of various methods of determining IDR. Three different methods were thoroughly investigated within the OrBiTo project and these were IDR determination based on (i) discs, (ii) coarse powder as received from the manufacturer (or physically ground using mortar and pestle), or (iii) suspensions in which a controlled particle size of the solid drug is dispersed in a fraction of dissolution medium (typically with some additional excipients to stabilize the suspension), producing a highly concentrated suspension that is then dispensed to additional dissolution medium (Fig. 1). Which method is most effective is governed mainly by the solubility of the compound. It has recently been shown that the disc method is suitable for compounds with apparent solubility $S_{app} > 1$ mg/mL, while the powder and/or suspension assays are recommended for compounds with $S_{app} < 100$ μg/mL [38,39]. Compounds that fall in the intermediate region can be studied with either of the methods. A good agreement

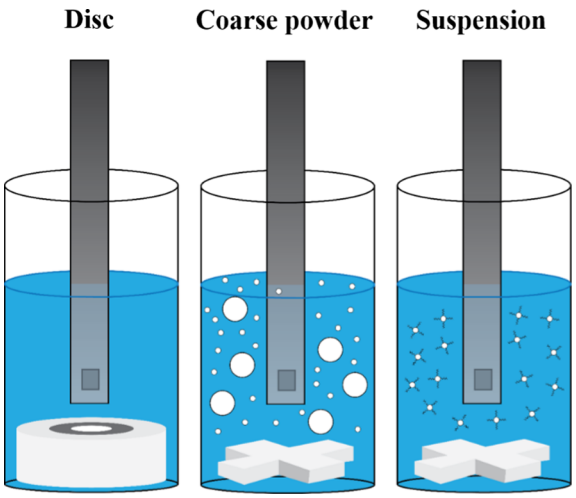

Fig. 1. Schematic of commonly used dissolution methods. The schematic illustrates the disc, coarse powder, and suspension methods as used in the μDiss Profiler with an *in situ* UV probe.

between powder intrinsic dissolution rate (PIDR) and disc intrinsic dissolution rate (DIDR) data has been shown ($r^2 = 0.97$ [40]). Although this direct comparison indicates that the two methods, based on flat surface of compact of disc versus curved surfaces of particles, are producing similar IDR values only 13 compounds were included in that comparison. In the work by Andersson et al., a direct comparison between the different methods was performed on additional six poorly water-soluble compounds. In that study, preprocessing the powder to a controlled suspension with particles in the sub-micron size range was required to produce similar dissolution values as those obtained by the disc method [39]. To conclude, more compounds need to be studied to understand the similarity and potential differences in the dissolution data obtained from different methods. Recent research efforts have focused on developing guidelines and experimental protocols especially for small-scale dissolution equipment to enhance intra- and inter-laboratory reproducibility of such solubility, dissolution, supersaturation, and precipitation measurements [38,41]. The sections below describe the three general methods in more detail.

2.1. Disc

In the disc method, the drug powder is compressed into discs of a fixed diameter. Theoretically, the result should be an exact and constant surface area that will be in contact with dissolution medium for the entire length of the experiment, and this putative consistency is a major advantage of this method [38]. However, a prerequisite for the method to work is that the surface will be completely smooth after compression. Furthermore, no loosely adhered material may be attached to the surface, and the dissolution must occur at the same rate over the entire disc so that the surface will remain smooth and without cavities. A rough surface would change the total surface area exposed to the dissolution medium during the course of the dissolution experiment and hence, the IDR would not be possible to calculate accurately.

The DIDR (μg/min/cm^2) is typically measured from rotating discs in dissolution media in either a traditional Wood's apparatus [36] or in miniaturized, commercially-available devices such as the μDISS Profiler [40], Sirius T3 [42] and Surface Dissolution Imaging (SDI) [43]. Flow-through cells have also been modified to include an online assessment of the solid phase during dissolution, e.g. with a Raman probe [44,45]. The DIDR can be calculated by the equation:

$$DIDR = \frac{dm}{dt}\frac{1}{A_{disc}} = V\frac{dc}{dt}\frac{1}{A_{disc}} \quad (4)$$

where m is mass (μg), t is time (min), A_{disc} is the disc surface area (cm^2), V is the volume of the medium (mL), and dc/dt is the slope of the straight line from the dissolution profile (μg/(min × mL)). In a small-scale apparatus, weight and volume are typically presented as μg and mL. The compression die used for rotational dissolution studies was originally developed by Wood et al. [36] (Fig. 2). In this method, 150–700 mg of pure compound is compressed by a hydraulic press, resulting in a disc with an exposed surface area of 0.5–1.3 cm^2 [37,46–48]. The compound disc can then be fitted to a traditional rotational assembly of a USP-type dissolution bath [48]. Dissolution over time is monitored by sampling from the bath and determining drug concentration *ex situ* with for example a UV spectrophotometer or HPLC. The sample preparation includes separation of potentially released but undissolved particles from the solution, which is commonly done by filtration.

A modified Wood's apparatus with a redesigned die cavity was proposed by Jashnani et al. [49,50] to minimize edge effects, yield a smoother, more compact drug surface, and prevent overcompression. The authors used the Levich prediction of dissolution rate as a function of disc rotation speed [51] in order to validate the results of their dissolution experiments. A Levich plot shows the available disc surface area divided by the dissolution rate (cm^2 s mg^{-1}) versus the reciprocal square root of rotation speed. The DIDR can then be determined from the reciprocal of the positive y-intercept of the plot, i.e. at infinite rotation speed in the absence of a stagnant layer [49]. IDR data obtained for albuterol using the modified disc apparatus more closely agreed with the prediction from the Levich plot ($r^2 = 0.90$) than did measurements using the original apparatus ($r^2 = 0.83$) [49]. More commonly, the Levich equation is used to estimate the effective boundary layer (h_{eff}) in disc dissolution experiments:

$$h_{eff} = 4.98\omega^{-1/2}\nu^{1/6}D_{eff}^{1/3} \quad (5)$$

where ω is the rotation speed (RPM), ν is the solvent kinematic viscosity and D_{eff} is the effective diffusivity (i.e. drug diffusion in the presence of micelles). For a typical drug compound with a diffusion coefficient of 10^{-3} m^2/s, the Levich boundary layer thickness is 0.05 mm at 100 RPM and 20 °C [52]. This boundary layer is not affected by the disc diameter

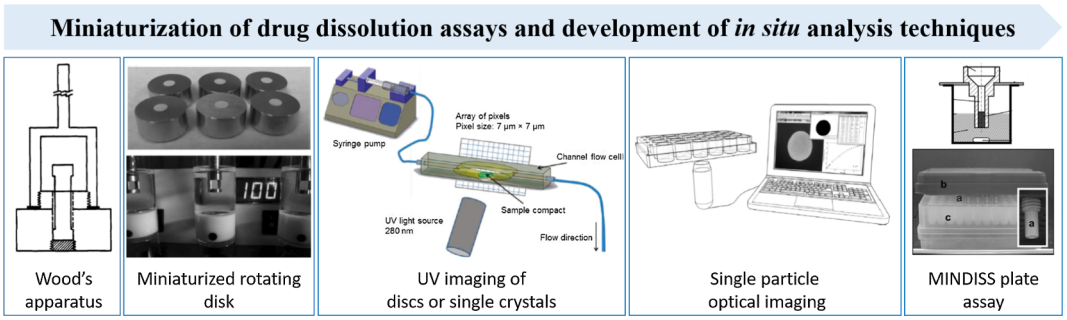

Fig. 2. Historical overview of developments in dissolution techniques highlighting their miniaturization as well as *in situ* sampling. *Reprinted with permission from* [36,37,57,113,115].

Table 1
Comparison of experimental conditions commonly used in particle-based or disc dissolution profiling assays.

Technique	Method		Sample amount	Area disc	Volume	Stirring	Temp.	Sampling		Detection	Ref.
	Particle-based	Disc	mg	cm^2	mL	RPM	°C	off-line	in-line	UV, HPLC, MS/MS	
MINDISS	✗	✓	2–5	0.0314	0.35	5–15 V[(1)]	RT/37	✓	✗	HPLC, (MS/MS)	[57]
µDISS Profiler	✓	✓	5	0.071	3–15	100	37 ± 0.5[(2)]	✓	✓	UV	[37,73]
SiriusT3	✓	✓	5–10	0.071	10–20	2700/ 4800	5–40	✗	✓	UV, pH-metric	[42,105]
inForm	✓	✓	5–100	0.071–0.503	20–80	100	10–70	✓	✓	UV, pH-metric	[127]
UV imaging	✗	✓	3–10	0.0314	0.56[(3)]	200 µL/min[(4)]	RT/37	✗	✓	UV	[113]
Single particle imaging	✓	✗	0.014–0.85	✗	3[(5)]	–	RT	✓	✓	optical, UV	[114,115]

[1]The stirring speed increases non-linearly with the voltage in the rotary magnetic tumble stirrer used.
[2]Temperature is externally controlled by a circulating water bath.
[3]Approximate cell volume of quartz channel flow cell.
[4]Imaging can be performed also in the absence of flow under static conditions.
[5] vol of one well in a 24-well plate.

and thus rotating disc experiments can be miniaturized.

Miniaturized DIDR equipment uses considerably smaller amounts of powder in the discs compared to the traditional Wood's apparatus (Table 1). In the commonly used µDISS Profiler, as little as 5 mg of compound is compressed in a Mini-IDR compression system with a resulting exposed disc area of 0.071 cm^2 [37,53]. These discs are fixed into a cylindrical Teflon rotating disk carrier and placed in a glass vial containing dissolution medium where drug concentration over time is monitored *in situ* using fiber optic UV probes [37] (Fig. 2). Several studies have demonstrated good agreement (r^2 = 0.99) between DIDR data measured by this miniaturized method and by the traditional Wood's apparatus [37,53]. Miniaturized disc assays have also been developed by physically scaling down traditional USP set-ups [54–56]. Alsenz et al. recently developed the Miniaturized INtrinsic DISsolution Screening (MINDISS) assay that uses a 2–5 mg disc with a surface area of 0.03 cm^2 placed in 96-well microtiter plates containing pre-dispensed dissolution medium [57] (Fig. 2). A reasonable correlation was found between the MINDISS method and the traditional large-scale Wood's apparatus (r^2 = 0.93–0.96). The MINDISS protocol is further described in Section 3.2.2.

Channel flow-through dissolution cells also maintain constant sample surface area and hydrodynamic conditions similar to rotating disk methods using small sample amounts (10–15 mg of drug). An advantage of the flow-through cells is that the dissolution medium is constantly exchanged, thus more easily guaranteeing sink conditions compared to closed beaker methods [58]. It also allows easy viewing of the solid during dissolution through a glass window mounted e.g. onto a microscope stage. The cell is designed to exhibit laminar flow conditions close to the surface of the drug compact with shear rates comparable to the rotating disk method. The dissolution rate of the drug can thus be determined using the following equation originally put forward by Nelson and Shah for convective diffusion [59,60]:

$$DR_{flow-throughcell,rectangular} = 0.808 D^{2/3} C_s \alpha^{1/3} b L^{2/3} \quad (6)$$

where DR is the dissolution rate, D the diffusion coefficient, C_s the solubility, α the shear rate over the dissolving surface, and b and L the height and the length of the compacted drug with rectangular surface, respectively. In case of a circular compact, the dissolution rate can be calculated using:

$$DR_{flow-throughcell,circular} = 2.157 D^{2/3} C_s \alpha^{1/3} r^{5/3} \quad (7)$$

where r is the radius of the compacted solid. Samples for e.g. HPLC analysis can be collected downstream of the flow-through cell. In recent years, the flow-through cells have mainly been explored for the online monitoring of dissolution as well as changes in solid state by e.g. UV–vis or Raman probes mounted at a glass window of the cell (see Section 3.4). For example, flow-through cells have been used to study solution-mediated phase transformations during dissolution of haloperidol [61].

Disc dissolution studies are mainly limited by compound solubility as well as the molar extinction coefficient (MEC) of the compound [38]. In particular, when using *in situ* UV probes, the drug concentration can drop below the detection limit of the probe for a long period during the measurement, which is the reason that disc assays in that type of setting are primarily recommended for compounds with S_{app} > 1 mg/mL [38]. However, highly sensitive analytics such as liquid chromatography coupled to concentration determination based on mass spectroscopy, allow also poorly soluble compounds to be measured based on the disc method. Yu et al. [46] investigated the effect of various experimental parameters (compression force, dissolution volume, distance of the drug disc from the bottom of the dissolution vessel, and disc rotational speed) on DIDR using Wood's set-up. The first three parameters were found to have no significant effect on measured DIDR, while the DIDR increased proportionally with the square root of the rotational speed, in agreement with theory based on the Levich equation [46]:

$$DIDR = 0.62\left(\frac{D^{2/3}\omega^{1/2}}{\nu^{1/6}}\right)C_s \quad (8)$$

The DIDR method was used to classify compounds according to the BCS with a suggested cut-off of 100 µg/min/cm^2 distinguishing soluble from poorly soluble compounds [46]. However, it should be noted that, when solubility is related to dose and the pH-range of 1–6.8 to distinguish between poorly soluble and soluble compounds (as e.g. in the BCS system) compounds might be defined as poorly soluble but still exceed the suggested cut-off of 100 µg/min/cm^2 in the medium used. Examples of such compounds are weak acids that have been defined as poorly soluble in the gastric compartment, but that have complete dissolution in the pH-range of the small intestine, where most of the absorption occurs. Hence, solubility in the particular dissolution medium should be used to help guide the choice of whether to use the disc method or one of the particle-based methods for determining IDR [39].

2.1.1. Characterization of discs

Wettability is a crucial parameter that can influence dissolution of compounds both in disc-based and particle-based methods [62]. The wetting angle between a liquid and a solid in the presence of a gas is described by the Young equation [63]. For pharmaceutical compounds, this measurement is most commonly determined by spread/sessile and capillary rise models [64], the former of which can be directly applied to compressed discs. A droplet is applied to the surface of the disc and the contact angle is recorded by a high-speed camera with image analysis software. However, wettability is also related to compaction pressure and surface roughness of the compounds, and these factors should therefore also be accounted for [65].

An additional characteristic is the compound's stickiness, which may result in difficulties in compressing powders to discs [39].

Typically, a fixed compaction pressure is applied during disc preparation; however, compounds with different compressibility and flowability can produce surfaces with different roughnesses, which in turn influences DIDR. Non-contact surface profilometry can be used to determine surface roughness [66] or surface porosity [65], and it has been proposed for characterizing discs prepared from compounds with poor compressibility before contact angle is determined [65].

Crystal habits (such as the favorable exposure of hydrophilic crystal facets) and crystal size will also greatly affect wetting and compaction behavior, which will in turn affect DIDR [67–69]. Raman spectroscopy can be used to study any changes in polymorphic form after compaction or even after the dissolution experiment [57,70]. For example, Alsenz et al. showed the appearance of testosterone hydrates after a disc dissolution experiment in FeSSIF [57]. Raman analysis can also be performed *in situ* using a Raman probe to monitor phase transformations occurring during dissolution [71]. Qiao et al. [71] studied solution mediated phase transformations of drug co-crystals during their dissolution from discs in order to understand the underlying mechanisms governing the measured DIDR. Wu et al. [72] used multi-wavelength UV imaging coupled with multivariate image analysis to map drug and excipient distribution in disc compacts as well as to detect any phase transformation that might have occurred during processing. This rapid imaging technique could be used to analyze disc properties in a high throughput manner, for instance as an in-process analytical quality control tool.

2.2. Powder

In powder dissolution assays, the solid compound is weighed directly into the vials used for the experiment, and dissolution medium (typically preheated to 37 °C) is added to initiate the experiment [7,73]. One advantage of powder compared to disc assays is that the significantly larger surface area available for dissolution results in much quicker measurements; typically, the powder assay measures IDR (PIDR) about 100 times faster than disc based assays [40]. Tsinman et al. [40] showed good agreement of PIDR compared to DIDR data obtained from both Wood's and miniaturized apparati. PIDR can be determined from the dissolution data without prior information about particle-specific surface area, shape, or size distribution, as particle size is directly estimated from the the amount of drug used and the dissolution curve (typically by fitting with a biexponential equation as described below) [40]. Avdeef et al. [73] used the Wang-Flanagan spherical particle non-sink equation to calculate particle size from powder dissolution data of five poorly soluble compounds and found good agreement with experimental measurements using a Coulter counter. The PIDR method can also be used to determine S_{app} if an excess amount of material is used, resulting in a saturated solution. Typically, 2–3 times more powder than the expected compound solubility value is added in powder assays [7]. However, the amount of powder that can be added is also compound and solubility dependent, since too large a fraction of undissolved powder particles may disturb assays that make use of, for example, *in situ* analysis (further discussed in Section 3). Powder assays can also be conducted using miniaturized equipment, using as little as 50 µg of compound in 1 mL of dissolution medium [73].

Mathematical models describing powder dissolution have been extensively studied over the past decades; a full account is beyond the scope of this paper, but the reader is referred to Dokoumetzidis and Macheras [74] for a comprehensive review. Powder dissolution data are typically fitted with a biexponential equation following Tinke et al. [75] assuming the presence of two particle size populations and a saturated solution at t = ∞ [7,38,40]:

$$C_{tot}(t) = C_0^{\infty}[1 - e^{-k_0(t-t_{LAG})}] + C_1^{\infty}[1 - e^{-k_1(t-t_{LAG})}] \quad (9)$$

where C_{tot} is the total concentration (typically provided as µg/mL when studying poorly water-soluble drugs) of the dissolved drug as a function of time t (min), C_0^{∞} and $C_1^{\infty}$are concentrations at $t = \infty$ from each of the two particle size populations (0 and 1), k_0 and k_1 (1/s) are rate constants, and t_{LAG} is the time (s) at which the dissolution starts. t_{LAG} corrects for experimental delays that can be caused by factors like poor wettability [7]. The initial derivative of this equation at $t = t_{LAG}$ is set equal to the limiting slope in the Nernst-Brünner equation:

$$\frac{dC_{tot}(t_{LAG})}{dt} = k_0 C_0^{\infty} + k_1 C_1^{\infty} = \frac{A_{app}}{V}\frac{D}{h_{app}}S \quad (10)$$

where A_{app} is the apparent total surface area of the compound under study (cm^2), h_{app} is the apparent thickness of the aqueous boundary layer (cm), D (cm^2/min) is the diffusivity of the compound in the medium used, V (cm^3) is the volume of the medium, and S (µg/mL) is the solubility of the compound. The ratio of A_{app} and h_{app} at the start of the dissolution is defined as:

$$\left(\frac{A_{app}}{h_{app}}\right) = \frac{V}{DS}(k_0 C_0^{\infty} + k_1 C_1^{\infty}) \quad (11)$$

When excess material is present, $S = C_0^{\infty} + C_1^{\infty}$. A nonlinear weighted regression analysis is used to determine C_0^{∞}, k_0, C_1^{∞}, k_1 and t_{LAG} associated with Eq. (9).

Powder dissolution data can be used to estimate DIDR [40]. For this purpose, the equation for disc intrinsic dissolution rate (DIDR, Eq. (4)), can be rewritten as:

$$DIDR = \frac{DR_{disc}^{max}}{A_{disc}} = \frac{1}{h_{disc}}DS \quad (12)$$

where DR_{disc}^{max} is the maximum disc dissolution rate. Similarly, this expression for PIDR can be expressed as:

$$PIDR = \frac{DR_{pwd}^{max}}{A_{app}} = \frac{1}{h_{app}}DS \quad (13)$$

with DR_{pwd}^{max} (µg/min) as the maximum slope in the powder dissolution curve. Eq. (13) can be substituted into Eq. (12) to eliminate the common term for dissolution rate, resulting in:

$$DIDR = DR_{pwd}^{max}\left(\frac{h_{app}}{A_{app}}\right)\frac{1}{h_{disc}} \quad (14)$$

The apparent h/A ratio is calculated from Eq. (11). The thickness of the aqueous boundary layer h_{disc} is estimated from the Levich equation (Eq. (5)). The diffusivity in Eq. (5) can be approximated with the empirical formula (at 37 °C):

$$D = 1.339 \cdot 10^{-4.15 - 0.448 \log MW} \quad (15)$$

where MW is the molecular weight of the compound. Eqs. (15), (11) and (5) are then inserted in Eq. (14) to yield the following expression to approximate DIDR using data obtained from powder measurements at 37 °C in an aqueous solution [40]:

$$DIDR = 0.0573\frac{DR_{pwd}^{max}}{V}MW^{-0.30}\sqrt{RPM}\left(\frac{C_0^{\infty} + C_1^{\infty}}{k_0 C_0^{\infty} + k_1 C_1^{\infty}}\right) \quad (16)$$

In biorelevant dissolution media, drugs diffuse in the presence of micelles and thus rather an "effective" diffusivity should be used, D_{eff} [7]. Eq. (16) can then be written in more general terms for biorelevant dissolution media at 37 °C:

$$DIDR = 0.460 D_{eff}^{2/3}\sqrt{RPM}\,(C_0^{\infty} + C_1^{\infty}) \quad (17)$$

2.3. Suspension

Dissolution measurements from particle suspensions rely on the addition of controlled suspensions, with particles of known surface areas, to the dissolution medium [39,76]. The controlled suspensions

are suspensions stabilized by the addition of low concentrations of polymers and/or surfactants (further described in Section 2.3.1). This results in well-dispersed suspensions, or, at least, easily redispersed suspensions if sedimentation occurs, which is an advantage over powder assays, where compound agglomeration in the dissolution media is often observed [73]. The Suspension Intrinsic Dissolution Rate (SIDR) can readily be calculated using:

$$SIDR = Vk\frac{1}{A} \tag{18}$$

where k is the initial slope of the dC/dt curve (concentration in μg/mL per time unit), V is the volume of the medium (mL), and A is the total particle surface area (cm^2). SIDR is only determined from the initial part of the dissolution curve where sink conditions apply with the assumption of constant particle size. The total particle surface area is calculated from a particle size measurement of the suspension by laser diffraction or DLS (see also Section 2.3.1), under the assumptions that particle size and number of particles are constant, and the particles are spherical. The volume of each particle is:

$$V_{particle} = \frac{4\pi r^3}{3} \tag{19}$$

where r is the mean radius of the particles in the suspension. The particle surface area is:

$$SA_{particle} = 4\pi r^2 \tag{20}$$

and the volume of compound added to the dissolution medium is:

$$V_{material} = \frac{m}{\rho} \tag{21}$$

where m is the total mass of compound added and ρ is the density of the compound. The total number of particles (n) in the suspension can thus be calculated from:

$$n_{particles} = \frac{V_{material}}{V_{particle}} \tag{22}$$

Finally, the total surface area (A, cm^2) of particles in the suspension added to the dissolution medium is calculated through [39]:

$$A = n_{particles} SA_{particle} \tag{23}$$

which can be used in Eq. (18) to determine SIDR. The suspensions typically come with some polydispersity. The surface area used for calculation can therefore be based on the mean value of the particle sizes measured in the sample, or the total surface area is calculated using size fractionation and the number of particles in each size fraction. For a small data set of six poorly water-soluble compounds, these two different ways of calculating the total surface area used for further IDR calculations did not result in significantly different results (Uppsala University, unpublished data). However, more compounds need to be studied to make general conclusions on how to best calculate the surface area of the suspension.

The main advantage of the suspension method, compared to the disc or powder methods, is the large and well-defined surface area exposed to the dissolution medium. The dissolution rate is thus high, and SIDR can rapidly be determined (Fig. 3). Furthermore, suspensions are often used in various preformulation and preclinical *in vitro* and *in vivo* trials, and the suspension dissolution method can be readily incorporated in the drug development process. It is important to have well-dispersed particles (that is, no agglomerates [77]) for such measurements, so that the primary particle size can be used in the interpretation of the dissolution data. Andersson et al. [39] demonstrated good agreement between DIDR and SIDR values for a series of poorly-water-soluble compounds using suspensions with particle size of about 1 μm. It should be noted that sometimes nanosuspensions tend to agglomerate as the stabilizing excipients become diluted in the dissolution medium. The suspension method appears to have an optimal range of particle size distribution, and that too small particles are not suitable for measuring IDR with this method.

2.3.1. Preparation and characterization of controlled suspensions

Particle suspensions can be prepared with classical top-down technologies such as the use of stirred media mills, planetary ball mills [78,79], ultrasonicators [80], or high-pressure homogenizers [81,82]. Suspension media typically contain surfactants and/or polymeric excipients that stabilize the particles by creating electrostatically repulsive or steric barriers, thereby preventing re-agglomeration [83,84]. Stabilizer type and concentration have significant effects on the resulting suspension particle size [79]. Common stabilizing excipients used for drug suspensions are polymers like hydroxypropylmethyl cellulose (HPMC) [78,81] and polyvinylpyrrolidone (PVP) [80], in combination with surfactants, like sodium dodecyl sulfate (SDS) [78], to improve wettability of the particles. Van Eerdenbrugh et al. carried out a screening study of excipients typically used in drug nanosuspensions [85]. In general, higher concentrations of stabilizing excipients improve suspension stability. The amount of surfactant adsorbed on the particle surface governs surface hydrophobicity [85]. Particle suspensions can be centrifuged to determine the non-adsorbed stabilizer concentration by for example NIR spectroscopy [86]. Electrophoretic measurements to determine the zeta potential also yield information about suspension stability at a certain pH, where stable suspensions have high zeta

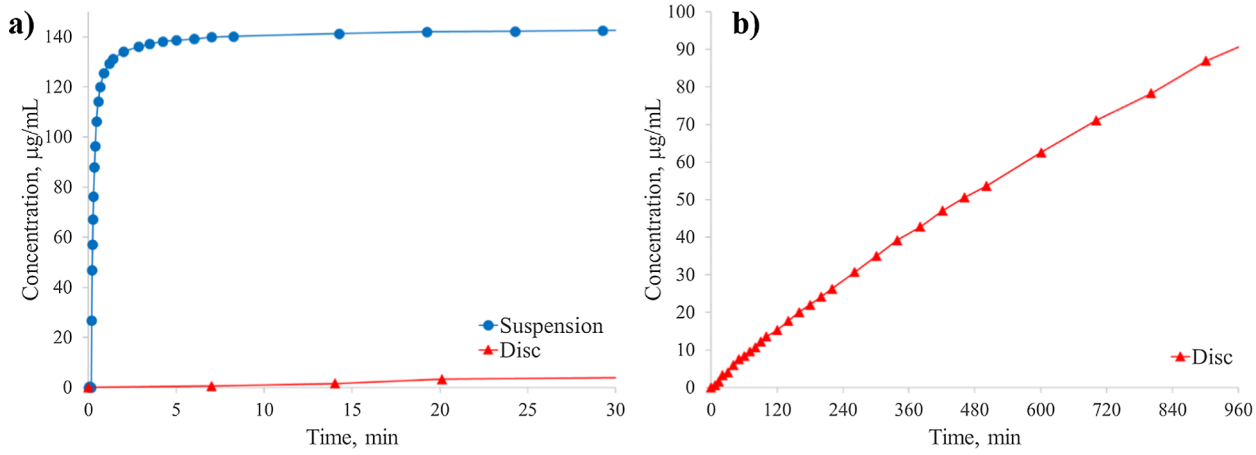

Fig. 3. Example dissolution profiles from disc and suspension assays. Dissolution profiles as a function of time for a poorly-soluble compound (carbamazepine) from controlled suspension (a, circles) and disc (a, b, triangles). The suspension method is completed within a few minutes (a), while the disc takes several hours (b). The presented data were obtained with the μDiss Profiler at 37 °C using biorelevant fasted state simulated intestinal fluid (FaSSIF version 1) as the dissolution medium.

potential values (positive or negative). Typically, the lowest possible concentration of excipient that still produces a controlled suspension is desired, in order to minimize effects of the excipients on the dissolution. The presence of surfactants at the dissolving particle surface can change the diffusion boundary layer thickness as well as surface kinetics [87], and thereby change the measured SIDR. Addition of surfactants to dissolution media above their critical micellar concentration (CMC) results in formation of micelles, which can significantly increase both S_{app} and IDR of poorly-soluble drugs [87]. Thus, for SIDR measurements, surfactant concentrations are typically kept as low as possible, resulting in solutions below CMC during the dissolution study [39,80]. If polymers are used, their adsorption to the particle surface reduces the surface area of the pure API that is interacting with the dissolution medium, which in turn also decreases the dissolution rate. It should be noted that long-term suspension stability is not a prerequisite for the SIDR assay, as freshly prepared suspensions are most often used during a work period of maximum a few days.

In the most commonly used bead-milling technology, the compound, predispersed in a stabilizer solution, is added to the milling chamber. The chamber is filled to 2/3 of its volume with ZrO_2 or Al_2O_3 beads, 0.4–0.8 mm in diameter [80,86]. Important milling parameters that will influence the resulting suspension particle size are milling time, rotation speed, the applied medium, and drug concentration. A gradual amorphization during milling might occur [88], and crystallinity should therefore be verified after milling and prior to dissolution measurements by for example X-ray diffraction (XRD), Raman spectroscopy, or differential scanning calorimetry (DSC). Raman spectroscopy has the advantage that it can measure phase changes occurring *in situ* during a dissolution assay by using dip probes connected via fiber optics to the spectrometer [89,90]. This method can also be used to determine the particle solid form(s) *in situ* in complex slurries [91,92]. However, the potential for using this method depends on the number of particles present. If the sensitivity is not high enough for *in situ* Raman, a concentration of the solid material through centrifugation of the suspensions would allow the pellet material to be explored with any of the mentioned off-line methods. Particle surface analysis can also be performed by X-ray photoelectron spectroscopy (XPS) to quantify the polymer or surfactant adsorption [88]. The suspension particle size is determined by dynamic light scattering (DLS) [39], laser diffraction, or visually by transmission electron microscopy (TEM) or scanning electron microscopy (SEM) images [80]. The latter imaging techniques also give information on particle shape, which can affect dissolution [76], and this factor is in fact neglected in most powder or suspension assays, which assume spherical particles. For TEM and SEM, it is important that a statistically relevant number of particles (> 100 particles) are measured to obtain representative particle size distributions. This step can be aided by image analysis software. The polydispersity index can also be determined from the particle size distribution and can be included in detailed dissolution analysis from polydisperse particle collections [93].

3. Determination of intrinsic dissolution rate

3.1. Hydrodynamics

Different approaches and equipment used will affect the hydrodynamics for dissolution. The most obvious parameter that affects hydrodynamics is medium stirring; the more efficient the stirring, the thinner the diffusion layer. The design of the dissolution apparatus will also play a role. For instance, Shiko et al. [94] demonstrated that, depending on flow rate and pump pulsation used in the USP4 flow-through cell, the flow can change from lamellar (low flow rate; 4 mL/min) to more heterogeneous and turbulent, with significant edge effects in the dissolution chamber (high flow rate, 16 mL/min). Stirring with magnets or paddles produces turbulence, and the flow depends on the geometry of the particular stirring device used. In a recent study by Johansson et al. [52], the hydrodynamics of the μDISS Profiler was explored with computational fluid dynamics (CFD). The shear rates and flow velocity were found to be significantly different depending on whether a cross magnet or a traditional stirring bar was used; furthermore, the position of the fiber optic probe also influenced these properties (Fig. 4). The conclusions were that positioning the probe off-center in the dissolution vial used by the equipment provided the best mixing of the dissolution medium, especially inside the probe head where the real-time determination of the concentration occurred.

CFD has also been used to establish the experimental conditions providing the same hydrodynamics in different equipment, enabling comparisons between different dissolution methods [95]. Stella et al. [96] compared a setting with 'perfect' lamellar flow to the three-dimensional flow of a rotating disc. In that study, a steady-state mass transfer model that incorporated convection, diffusion, and ionization processes (for charged APIs) was developed to better calculate effects relevant to physiological conditions.

Attempts to link *in vitro* to *in vivo* performance were made by Lindfors et al. [97], who performed CFD simulations to understand which factor (hydrodynamic effects or wetting effects) was governing the dissolution of felodipine, a poorly water-soluble, highly lipophilic drug, when exposed to the small intestine. Felodipine suspension was studied in a USP II apparatus at two different paddle speeds (25 and 200 RPM) and with increasing surfactant concentration (although keeping the concentration below the CMC). The experiments were complemented with CFD simulations, where calculations of the dissolution kinetics were performed using a quasi-steady-state approximation where the different paddle speeds were accounted for via the Peclet (Pe) number [97]:

$$\frac{dR}{dt} = \frac{DV_m}{R}(C_b - C_S)(1 + Pe)^{0.285} \quad (24)$$

where R is the particle radius, D is the monomer diffusion coefficient in the solvent, V_m is the molar volume and C_S and C_b are molar concentrations for saturation solubility and bulk concentration, respectively. The Peclet number is a dimensionless number that is defined as

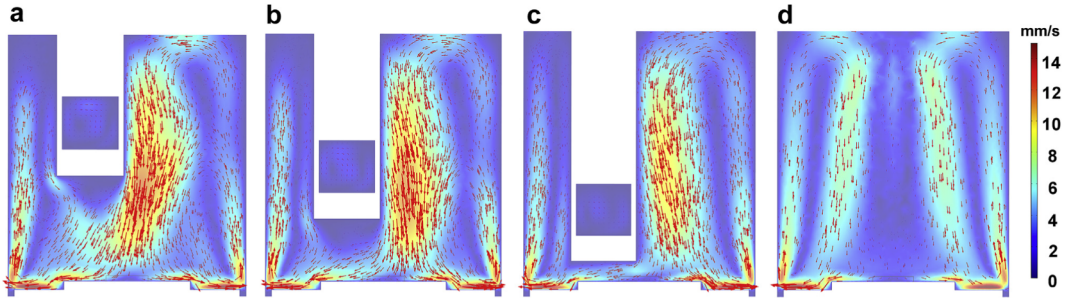

Fig. 4. CFD simulations of hydrodynamics in a miniaturized dissolution apparatus (μDiss Profiler) showing flow near the disc and mixing of the dissolution medium. The simulations show the disk stirrer at 100 RPM with three axial probe positions (a–c) and without a probe (d). *Reprinted with permission from* [52].

the ratio between advection of a solute by the flow to the rate of diffusion of the same solute as dependent on a gradient. It can be calculated by the product of the Reynolds number (which relates to flow type; low Reynolds number defines laminar flow whereas high number defines turbulent) and the Schmidt number (the ratio beween kinematic viscosity and mass diffusivity):

$$Pe = \frac{2gR^3\Delta\rho}{9D\eta} \quad (25)$$

where g is the gravitational acceleration, Δρ the density difference between the particles and the media and η the media viscosity. The different shear stress values obtained when changing the paddle speed did not affect the dissolution rate, and it was concluded that dissolution *in vivo* would not be affected by hydrodynamics; rather, dissolution was affected by the amount of solubilizing agents present.

The above given examples were only a few of the recent studies linking hydrodynamics and experimental settings to dissolution. In the following section, a number of commonly used techniques will be presented in more detail with an overview of the experimental conditions in Table 1. Focus is on recently developed equipment and its potential use for IDR measurements; for this reason, classical USP methods and the Wood's apparatus (and variants thereof) are not covered. A good complement to this review is the article on analytical technologies for small-scale dissolution and precipitation testing by Kuentz [89].

3.2. Off-line determination of concentration changes

3.2.1. Miniaturized dissolution vessels and flow-through cells

Miniaturized dissolution vessels and flow-through cells are commonly custom-built to produce the desired hydrodynamics, allow connection to different detection sources, and/or allow for a general flexibility of the system, and there is no standard protocol for these types of studies. Miniaturized dissolution vessels and flow-through cells can be connected to an off-line analysis for which samples are taken at particular time intervals, filtered and analyzed by UV/FL-plate readers or HPLC-UV(-MS/MS) (the preferred analytical tool depends on the sample concentration generated). The off-line measurement should be performed directly after the sample is taken. A drawback of off-line measurements and sample preparation factors (like filtration) is that these may affect the samples. In particular, filtration may result in adsorption of the dissolved material to the filter material, thereby artificially lowering the concentration measured. Some flow-through cells are therefore coupled to a UV cuvette positioned off-centered from the analyte (e.g., the disc), and this approach requires less sample preparation; i.e. the samples are analysed downstream the disc without need for pipetting, filtration and sample preparation to allow concentration determination [44,98]. Currently, several flow-through cells may be coupled to direct measurement of the concentration, and these methods are described below. For the miniaturized dissolution vessels (as well as larger USP baths), flexible fiber optic probe systems have transformed the traditional off-line measurements into *in situ* (UV) measurements.

3.2.2. Microtiter plate-based methods for determining intrinsic dissolution: MINDISS

The MINDISS method is an attempt to adjust IDR measurements to the setting commonly used in late discovery/early development stages [57]. At these stages, experimental protocols require an approach based on small amounts of material and, if possible, high-throughput automation to allow screening for suitable excipients. With such a set-up, a larger number of dissolution media could be explored to provide a better understanding of how factors like intestinal fluid(s) will affect the dissolution of the drug, which will in turn affect its formulation.

The MINDISS assay is a response to these demands. MINDISS is performed in a 96-well flat-bottomed polypropylene plate. The drug compact is produced by compressing 2–5 mg of the API into custom-made holders of 2 mm diameter using a compaction pressure of 5 kg/0.0314 cm^2. The holders are immersed in 0.35 mL of dissolution medium that has been dispensed automatically into the carrier plate. The disc side of the holder is face down and the dissolution medium is stirred by a tumble stirrer. At predefined time intervals, the sample holders are transferred to a new plate with predispensed dissolution medium. The samples in the previous plate are filtered through a 0.45 μm hydrophilic, low-protein binding filter (to reduce potential adsorption), and subsequently measured with UPLC (UV detection). The transfer setup allows the medium that the disc is exposed to during the assay to easily be changed, and one can therefore perform a classical 'gastric to small intestine transfer' experiment using the same disc. Although this method was not fully automated when published by Alsenz et al. [57], it has a relatively high throughput and can handle 48 discs per day in its semi-automated version.

3.3. In situ determination of drug dissolution

3.3.1. The μDISS Profiler

In the OrBiTo project the μDISS Profiler has been a key instrument that was evaluated for its use in dissolution, solubility, supersaturation and precipitation measurements in the early drug development stage; this instrument was identified as the most common small scale dissolution system used by the different industrial partners involved in OrBiTo. The μDISS Profiler uses *in situ* fiber optic probes that monitor amounts of drug dissolved through UV absorbance spectroscopy (200–780 nm); hence, a prerequisite for its use it that the compound under study has a chromophore. Typical volumes range from 3 to 15 mL, and a variety of biorelevant dissolution media have been shown compatible with this analytical method [7,99,100]. The *in situ* probes have flexible tips, and the user can chose path lengths from 1 to 20 mm. The optimal path length depends on the concentration expected to be measured and the sensitivity of the chromophore of the compound under study. Magnetic stirrers are used, producing a turbulent flow and, as described in Section 3.1., the type of magnetic stirrer will produce different hydrodynamic conditions. Stirring speed is adjusted manually at the initiation of the measurement. Typically, 100 RPM are used for dissolution studies, but up to 800 RPM can be used, which is common when establishing the standard curve. The μDISS Profiler has eight parallel fiber-optic probes, each of which is calibrated by its own standard curve. The user may choose to use each of the probes to study a particular condition, or several of the probes to obtain replicates during the same experiment. The equipment is compatible with both disc and particle-based assays (both coarse powder and suspensions). Mathematical filtering making use of the 2nd derivative of the absorbance spectra collected is used to enable particle-based studies and reduce the disturbance of particles on the absorbance spectrum. Depending on which assay is performed and the expected dissolution rate of the compound, measurements can be made as often as every 2 s. If the user is also interested in solubility, the experiment can be designed to measure that property as well; for such experiments the compound needs to be added in excess to allow the saturated concentration to be reached. Recently, the μDISS Profiler has also been used to study supersaturation and precipitation pattern [41,101], the effect of different excipients on dissolution and absorption processes [102,103], and the instant release from particle-rich formulations [104].

A standard protocol for how to use the μDISS Profiler for IDR has recently been published, so the work flow is only briefly described here [38]. The user starts the experiment by calibrating each of the probes. To produce the standard curve, a stock solution prepared in a cosolvent (commonly dimethylsulfoxide or methanol) is aliquoted into the dissolution medium, stirred well (800 RPM, 1 min), and measured for absorbance. The final concentration of the cosolvent should be kept low so as not to influence the UV read out (a concentration < 1.5 v/v% is

preferred). The standard curve is prepared in 3 mL vials, while the IDR of the compound of interest is often determined using 15 mL of solvent. The start of an experiment depends on whether a disc, coarse powder, or suspension study will be performed. For a disc study, 5–10 mg of powder is compressed into a magnetic disc holder, which is then placed in the vial. For a powder assay, the powder is weighed into each vial and a magnetic stir bar is added to the vial. For both disc and powder assays, the experiment starts when the dissolution medium is added to the dissolution vial and stirring commences. For controlled suspension studies, the dissolution medium is added to the vial, stirring commences, and the experiment begins when an aliquot of the suspension is added to the dissolution medium. The time needed for the experiment depends on the method, and termination of the experiment can be guided by real-time data.

3.3.2. The SiriusT3 and inForm

The SiriusT3 and inForm instruments are further examples of equipment that has been developed to understand small-scale (low volume) dissolution behavior of samples [42,105,106]. Both are automated titration systems with built-in pH control and UV fiber-optic probes allowing for direct *in situ* monitoring of dissolving drugs over time from UV absorbance spectroscopy. The SiriusT3 typically uses 10–20 mL of buffer medium dispensed manually into the dissolution vessel containing the sample, and UV data collection is initiated by the user. The fiber-optic probe has a fixed 10 mm pathlength window. The inForm instrument is automated and contains dispensers for volumetrically dispensing reagents via capillaries into the measurement vessel. The dissolution medium typically consists of 40 mL of buffer dispensed and adjusted to the starting pH. The instrument uses a robotic arm to automatically lower samples like discs into the buffer solution, allowing instantaneous UV data collection upon sample introduction. The mini fiber-optic probe is adjustable with 1, 2, 5, 10, or 20 mm pathlength windows. The medium in the dissolution experiments is stirred at a constant rate throughout the dissolution experiment. UV–visible absorption spectra are recorded via a fiber-optic dip probe with a diode array spectrophotometer (200–700 nm) at fixed intervals for a specified period, in order to determine the amount of drug appearing in the dissolution medium. In disc dissolution experiments, UV spectra are typically recorded every 30 s for 2 h.

Discs are prepared for SiriusT3 by pressing 5–10 mg of compound into 3 mm diameter discs and the resulting minitablets are visually examined to ensure their surfaces are smooth and free of visible defects and free powder. The discs are then placed in holders and held in place by an O-ring seal, which prevents exposure of the reverse side of the disc to the dissolution medium, resulting in a total exposed surface area of 0.07 cm^2. The disc holder is inserted into an appropriate-sized dissolution vial.

For the inForm, samples can similarly be prepared as discs with 3, 6, or 8 mm diameters (Fig. 5). The minitablets are compressed into the cylindrical depression in the face of the steel disc holder. The reverse side of the disc is sealed with a rubber bung to prevent exposure to the dissolution medium, resulting in total exposed surface areas of 0.07, 0.28 or 0.50 cm^2 respectively. As mentioned above, the discs are automatically picked up and lowered into the dissolution vial using a robotic arm once the dissolution medium has been prepared.

Fig. 5. inForm discs allowing for a defined surface area to be presented to the dissolution medium for IDR measurement.

Both powders and suspensions can be studied with SiriusT3 and inForm. For the SiriusT3, buffer medium is dispensed manually into the dissolution vessel containing the sample and UV data collection is initiated by the user. The inForm instrument uses a robotic arm to automatically introduce the sample (e.g., powder inside a basket) into the buffer solution, or suspensions can be directly introduced via a liquid-handling needle. Instantaneous UV data collection is triggered upon sample introduction. The frequency of recorded spectra and experiment duration is easily modified to suit the needs of the experiment; for instance, UV spectrum can be recorded every few seconds.

To determine the dissolution behavior of a compound, UV absorption data is converted to absolute sample weights using the pH-dependent, MECs that have previously been determined using the SiriusT3 or inForm. MECs and pKas of all compounds studied are determined in advance by UV-metric titration, and sample concentrations are optimized in order to obtain a peak UV absorbance of approximately one absorbance unit. Where possible, titrations are carried out under aqueous conditions; however, some poorly water-soluble compounds may require methanol as cosolvent. MECs are determined at multiple wavelengths and used to convert UV absorbance data from the dissolution assay directly into sample concentrations. Depending on the substance, a suitable wavelength region is selected during data treatment, and a regression algorithm applied to determine dissolved concentration in solution. For poorly soluble substances, a sensitive wavelength region is typically chosen (i.e., high MEC region to enhance sensitivity for low amounts of dissolved material). For rapidly dissolving compounds, it is possible that the absorbance signal may become too high; that is, at high drug concentrations, no light reaches the detector. Under these conditions, the Beer-Lambert law is not obeyed and UV absorbance may not follow a linear response with sample concentration. Hence, analytical wavelength regions are typically selected so that any data corresponding to saturation of the UV light source are excluded from the calculation (e.g., > 1.2 absorbance units). The light pathlengths (1, 2, 5, 10 or 20 mm) for the fiber-optic probes on the inForm can be adjusted for optimal sensitivity.

3.4. Imaging-based methods for dissolution determination

3.4.1. UV–VIS imaging

The application of UV–VIS imaging for dissolution has recently been comprehensively reviewed by Østergaard et al. [107]. The UV–VIS imager is a flexible system that can be combined with different custom-built flow-through cells, and it is also commercially available (e.g., D100 from Paraytec, UK and SDi from Pion Inc, USA) [43,108]. These cells can readily be coupled with *in situ* Raman spectroscopy to also study phase transformation events that could occur during dissolution (Fig. 6a–c) [71,109,110]. Set-ups have also been developed that allow the simultaneous use of UV imaging and *in situ* Raman spectroscopy during dissolution [111,112]. The technique is used to analyze the surface of an API disc or simpler mixes of excipients and API. The advantage of UV–VIS imaging is that it generates spatially and temporally resolved absorbance maps (contour-plots), which by the use of the Beer-Lambert law can be transformed into concentration maps. Direct measurement on the surface of the dissolving material further allows for measurement of processes occurring at the solid-solvent interface, in contrast to the methods discussed above, which measure concentrations in the bulk [113]. Hence, not only dissolution can be studied by this method, but also effects such as compact swelling, supersaturation/precipitation at the solid-solvent interface, and partitioning of the API into different phases can be revealed.

Because the UV–VIS imaging technique can be combined with many different types of experimental set-ups, a single description of how IDR is determined is difficult to provide. However, important factors to keep in mind include (i) determining noise obtained from the dissolution medium itself (i.e., information of the blank measurement must be included), and (ii) imaging resolution, which depends on the grid system

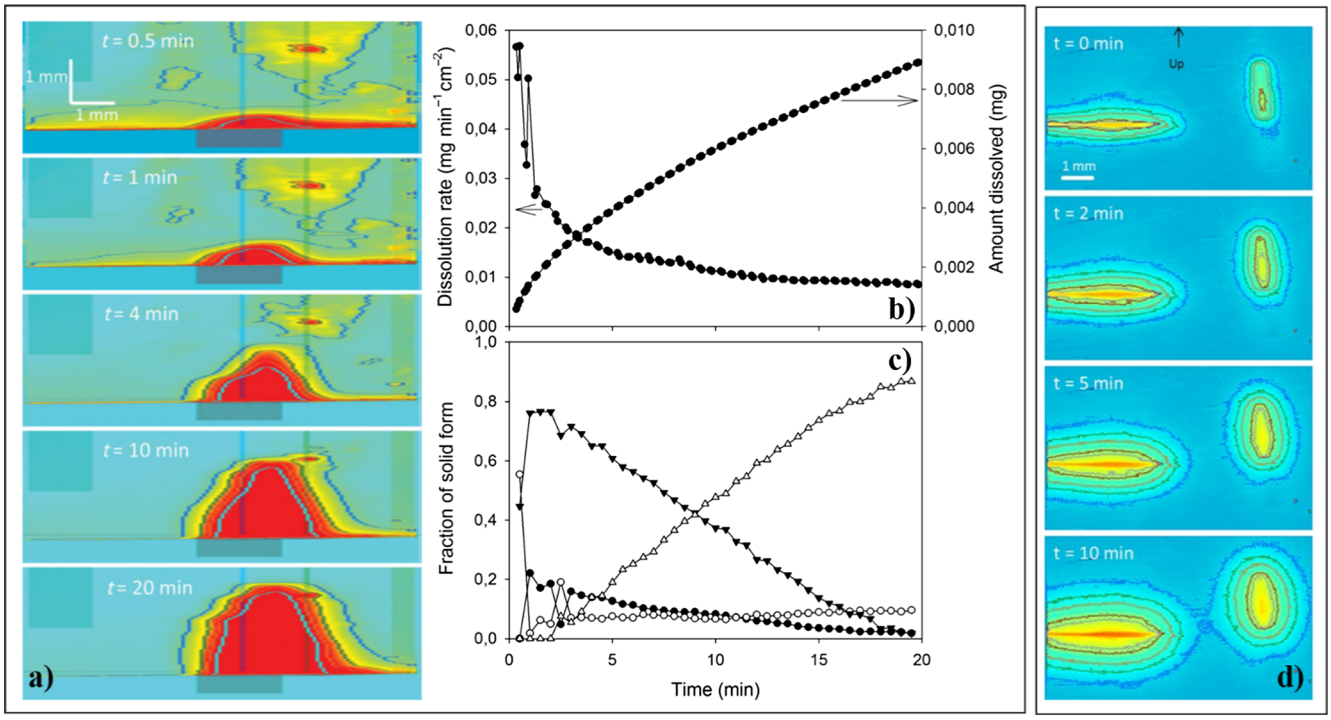

Fig. 6. UV imaging of discs or single crystals for studying the dissolution behavior of an API. UV absorbance maps visualizing the progress of dissolution of sodium naproxen from compacted discs in 0.1 M HCl at ambient temperature (a) and the corresponding dissolution rate and cumulated amount of dissolved naproxen as calculated by image analysis (b). The phase transformation of sodium naproxen into three different intermediate solid forms during the flow-through dissolution experiment was quantified with an *in situ* Raman probe (c). Precipitation of a solid naproxen form was observed during the imaging of (a). Absorbance contour maps of the dissolution of lidocaine crystals in 0.5% (w/v) agarose gel at pH 7.4 as a function of time (d). *Reprinted with permission from* [108,111].

used for pixels (whether pixels are binned at for instance 1 × 1 or 4 × 4 per grid). The grid is used to understand the background signal from e.g. cover slips and blank dissolution medium as well as the crystal form of the drug and the impact of density on dissolution/diffusion. Nielsen et al. [110] reported that dissolution rates of four furosemide forms determined in a UV imaging system were consistent with those obtained in a μDISS Profiler disc experiment.

3.4.2. Particle and single crystal dissolution microscopy

Single crystal dissolution imaging (Fig. 6d) is useful for understanding crystal dissolution in a more mechanistic manner. This method can measure crystal growth as well as reveal spatial differences in dissolution of a crystalline form. Recently, a combination of surface characterization tools and microscopy has been developed to analyze dissolution (and crystal growth) of particles. In a series of papers, Svanbäck et al. [114–116] explored optical microscopy as a tool for determining solubility and dissolution, including IDR. They performed the IDR experiments by mounting a single particle of the API in a 3D-printed flow-through vortex trap. Images of the dissolving, rotating particle were acquired through a magnifying lens by a complementary metal–oxide–semiconductor (CMOS) image sensor using stroboscopic illumination of the particle. Image analysis was then applied to calculate equivalent sphere volume and surface areas as a function of time. Svanbäck et al. studied a series of compounds covering more than four orders of magnitude in IDR values, taking little time (assays were completed within minutes) and using as little as 14–747 μg (particle sizes of 136–590 μm) of material. The IDR data showed excellent correlation with literature equilibrium solubility ($r^2 = 0.999$), which the authors used as a surrogate for IDR, arguing the strong connection between the two properties. This method seems very promising, but larger datasets and data relating the single particle method to more traditional methods available are warranted.

Like the single particle assay, single crystal assays for studying dissolution are available. These are useful for understanding differences in dissolution patterns (as well as crystal growth pattern in the presence of a supersaturated solution) between different crystal forms [117,118]. The size of the crystal, as determined by microscopy, can be used to determine the IDR. A difficulty with the technique is that it requires growing a perfect crystal, large enough to be measured by microscopy. The measurement techniques have made use of atomic force microscopy (AFM), typically coupled to a flow-through cell [119–121]. AFM probe parameters such as the cantilever size, the tip cone height, and the cone angle all influence the measurement of mass transport at the reactive surface under study [122]. To minimize disturbance of mass transport at the reactive substrate's surface (here, the surface of the crystal), the cantilever radius should be small, the tip cone should be long, and the cone angle should be kept low. The tip probe has the potential to disturb the flow, and therefore the diffusion and dissolution process, which can be solved by optimizing the geometry and position of the AFM tip probe.

Various types of imaging have also been used to study single crystals. Østergaard et al. [123] used static conditions to study dissolution of lidocaine at pH 7.4 after mounting a single crystal into a dissolution cell which was connected to an ActiPix SDI300 dissolution imaging system. Image analysis was then dependent on a pixel grid system and number of images taken. A total surface area of 9 × 5.5 mm^2 was studied using 7 × 7 μm^2 pixels binned 4 × 4, with 2.3–2.6 images recorded per second for image analysis. In a recent study by Clark et al. [124], a 3D analysis of crystal dissolution and growth was performed using Bragg coherent diffraction imaging (BCDI). A coherent X-ray diffraction pattern was collected from all parts of the crystal and was used to generate the crystal morphology. Single calcite crystals (< 2 μm) were monitored while they underwent cycles of crystal growth and crystal dissolution. The image analysis revealed that although the entire surface of the calcite was involved in the dissolution, the rate was higher at particular points. This uneveness resulted in increased surface

Table 2
Typical application of IDR methods in industry.

Method	Application	Stage
Disc	• IDR as compound property of respective solid state form • Changes of solid state form during contact with aqueous media	Research
Coarse powder	• Influence of different media • Screening of excipients	Early development
Suspension	• Determination of target particle size	Early development

roughness and, subsequently, increased specific surface area, which should be used to calculate the IDR. However, the suitability of BCDI for studies of dissolution of drug-like compounds remains to be shown.

4. Industrial applications for IDR data

In the OrBiTo project IDR is one of the physicochemical properties that has achieved significant attention; both the role of this property in the early drug development of the pharmaceutical industry as well as feasible methods to be used at this stage to determine IDR have been in focus. When profiling a candidate molecule for its biopharmaceutical properties (Table 2), attention is typically focused on properties such as permeability and thermodynamic equilibrium solubility (across the physiological pH range and/or with biorelevant media). From an industrial point of view, the IDR is important to measure for compounds that suffer from dissolution rate limited and solubility limited absorption to better understand formulation aspects that may allow the API to completely dissolve during the transit time of the small intestine. The IDR of a molecule is very useful during solid form selection, and IDR datasets are often used to support the selection of a preferred salt, co-crystal or polymorph [87]. Measurement of IDR can be more informative and discriminatory in comparison to the simple shake flask equilibrium solubility values, which can be misleading when assessing the performance of different salts or the effect of formulation excipients on API dissolution. IDR has also been used to study the effect of crystal surface chemistry on API dissolution [67]. For poorly water-soluble molecules requiring a bioenhanced approach, IDR may be used to guide the selection of an enabling technology by measuring the dissolution rate improvement achievable with API solid dispersion [125,126] or cyclodextrin [127] formulations. Another important parameter for formulation development is information on what particle size would theoretically be needed to obtain dissolution of a given dose in a time range equal to the small intestinal transit time; this particle size can be estimated by IDR measurements combined with *in silico* modeling. Knowing the optimal particle size can help the formulator decide whether the compound should be formulated in a conventional dosage form, or if an enabling technology would be needed, depending upon the physical feasibility of obtaining the theoretical calculated particle size.

During the early development phase, availability of an API is often constrained and IDR approaches need to be parsimonious with material, preferably using just a few milligrams (mgs) of compound, while still obtaining reliable data. For this reason, methods like the traditional Woods apparatus are not feasible since too much material would be required for the measuremet. The lack of material also make proper particle size evaluation of the solid not feasible. Several methods have been developed to meet this need with the single particle IDR optical imaging method developed by Svanbäck et al. [114] potentially generating IDR data (and other key physicochemical properties) with just a few mgs of API. The surface dissolution imaging technique developed by Sirius/Paraytec [43,107] can determine IDR with around 3–10 mgs of API and can also be used to determine an experimental value for the diffusion coefficient [128]. The controlled suspension approach has also been proposed as a material-sparing rapid technique for determining IDR [39]. Perhaps the most commonly used approach in an early-development setting is to measure IDR using the μDiss equipment, because it uses relatively small quantities of API while still producing data comparable to those produced by the traditional Wood's apparatus [37,53].

Regardless of the method and technique employed to obtain experimental IDR data, the use of IDR to make decisions during development can be surprisingly complex. Considering the application of IDR during solid form screening (salt, co-crystal, or polymorph), datasets are typically used in a qualitative, comparative context, and selection is often determined on a simple rank-ordering of the solid forms of interest. The same applies for comparing compounds being investigated in cases where IDR values are used as a selection criterion. The scientific challenge is to select the IDR that will provide robust *in vivo* performance for the particle size range achievable for the molecule. In terms of salt selection, this decision is not always as straightforward as selecting the compound with the highest dissolution rate. Even if all other considerations are equal (stability, crystallization tendency, crystal habit etc.), the dissolution rate needs to be considered in the context of *in vivo* performance. A very high dissolution rate, while superficially attractive, may generate an unstable, too highly supersaturated phase which ultimately may drive uncontrolled precipitation of the molecule in the gastric or intestinal regions of the GI tract. Thus, permeability needs to be considered as well. It is clear that using IDR data can be complicated by this consideration, and further dissolution approaches, like the artificial stomach duodenum model or similar gastrointestinal transfer technologies [129], may be needed to fully elucidate the resulting bioperformance.

When determining the influence of IDR on dissolution performance, it is important to remember to account for the contribution of a particular API's achieveable particle size to the dissolution profile. Calculating dissolution times in various media based on both an API's IDR and particle size allows the formulation scientist to determine whether a particular solid form is adequate from a bioperformance perspective. It is also important to consider the effect of an unexpected crystal form change on dissolution, and bioperformance of the drug product. For example, a form change to a hydrate can often result in a significant reduction in IDR, yet the effect on formulation performance will depend on multiple factors (particle size, dose, biorelevant solubility, permeability), all of which need to be fully considered to determine the impact of such a change. From an industrial perspective IDR is also used for quality control during late stage development, and dissolution properties of the API are recharacterized after a change in the supplier or manufacturing site.

Several authors have proposed using IDR [46,130] or apparent dissolution data [131,132] (which uses a micronisation process to effectively normalise the effect of differing surface areas in different APIs) in the context of a biopharmaceutics risk assessment. These studies have proposed that IDR as a rate phenomenon like permeability might correlate better with *in vivo* drug dissolution than static equilibrium solubility measurements. The two studies [46,130] that have used IDR data to classify a series of passively absorbed model compound sets showed a good relationship between IDR and BCS solubility classification. However, establishing a suitable boundary descriptor that could be used to robustly classify compounds with dissolution limitations is complicated by the hydrodynamic conditions of the test, which need to be considered for the technique used to experimentally determine IDR values [133]. As described by Andersson et al. [38], a strict protocol needs to be followed to allow interlaboratory comparison and so that *in vitro-in vivo* results can be reliably correlated with each other.

5. Summary

This review provides an updated view on the use of IDR in the context of early-stage drug development. The number of methods that have been developed in the last decade and the sophistication of these

methods enables measuring IDR using small amounts of material (μg to lower mg scale), with simultaneous assessments of possible solid state transformations. An increased understanding of the hydrodynamics of these experiments and how those are related to classical dissolution equipment (USP-type) and *in vivo* conditions has been gained. CFD calculations will be a useful tool for future exploration of *in vitro-in vivo* correlations from a hydrodynamic point of view. To improve understanding of how dissolution rate affects absorption of a given drug, combinations of different tools, e.g. combined dissolution and permeation, and release, dissolution and permeation tools, have emerged. From an industrial perspective, IDR continues to be an important property to measure during salt and formulation selection, to understand biorelevant dissolution of the API, and as a quality marker of the API during later stage development and API production. It is expected that in the near future IDR measurements will be, by default, connected to analysis of possible solid state changes. Currently, these two measurements are performed in a flexible manner and the addition of a solid state characterization technique to the dissolution measurement is typically an add-on option that particular laboratories utilize. Further development of image analysis will facilitate methods that build on crystal or particle-based methods coupled to different imaging techniques. This development will further help us to understand the processes that occur at the surface-solvent interface, rather than analyzing bulk phenomena, which is the main focus of IDR studies today.

Acknowledgements

This work has received support from the Innovative Medicines Initiative Joint Undertaking (http://www.imi.europa.eu) under grant agreement no. 115369, resources of which are composed of financial contributions from the European Union's Seventh Framework Programme (FP7/2007-2013) and EFPIA companies.

Conflicts of interest

K. Box is an employee of Pion Inc (UK) Ltd.

References

[1] G.L. Amidon, H. Lennernas, V.P. Shah, J.R. Crison, A theoretical basis for a biopharmaceutic drug classification: the correlation of in vitro drug product dissolution and in vivo bioavailability, Pharm. Res. 12 (1995) 413–420.
[2] M.S. Ku, Use of the biopharmaceutical classification system in early drug development, AAPS J. 10 (2008) 208–212.
[3] L.Z. Benet, C. Wu, J.M. Custodio, Predicting drug absorption and the effects of food on oral bioavailability, Bull. Tech. Gattefossé 99 (2006) 9–16.
[4] B.J. Krieg, S.M. Taghavi, G.L. Amidon, G.E. Amidon, In vivo predictive dissolution: comparing the effect of bicarbonate and phosphate buffer on the dissolution of weak acids and weak bases, J. Pharm. Sci. 104 (2015) 2894–2904.
[5] B. Hens, Y. Tsume, M. Bermejo, P. Paixao, M.J. Koenigsknecht, J.R. Baker, W.L. Hasler, R. Lionberger, J. Fan, J. Dickens, K. Shedden, B. Wen, J. Wysocki, R. Loebenberg, A. Lee, A. Frances, G. Amidon, A. Yu, G. Benninghoff, N. Salehi, A. Talattof, D. Sun, G.L. Amidon, Low buffer capacity and alternating motility along the human gastrointestinal tract: implications for in vivo dissolution and absorption of ionizable drugs, Mol. Pharm. 14 (2017) 4281–4294.
[6] J.J. Sheng, D.P. McNamara, G.L. Amidon, Toward an in vivo dissolution methodology: a comparison of phosphate and bicarbonate buffers, Mol. Pharm. 6 (2009) 29–39.
[7] J.H. Fagerberg, O. Tsinman, N. Sun, K. Tsinman, A. Avdeef, C.A.S. Bergström, Dissolution rate and apparent solubility of poorly soluble drugs in biorelevant dissolution media, Mol. Pharm. 7 (2010) 1419–1430.
[8] J.B. Dressman, C. Reppas, In vitro-in vivo correlations for lipophilic, poorly water-soluble drugs, Eur. J. Pharm. Sci. 11 (2000) S73–S80.
[9] E.D. Gamsiz, M. Ashtikar, J. Crison, W. Woltosz, M.B. Bolger, R.L. Carrier, Predicting the effect of fed-state intestinal contents on drug dissolution, Pharm. Res. 27 (2010) 2646–2656.
[10] G. Ottaviani, D.J. Gosling, C. Patissier, S. Rodde, L.P. Zhou, B. Faller, What is modulating solubility in simulated intestinal fluids? Eur. J. Pharm. Sci. 41 (2010) 452–457.
[11] E. Soderlind, E. Karlsson, A. Carlsson, R. Kong, A. Lenz, S. Lindborg, J.J. Sheng, Simulating fasted human intestinal fluids: understanding the roles of lecithin and bile acids, Mol. Pharm. 7 (2010) 1498–1507.
[12] Y. Tsume, D.M. Mudie, P. Langguth, G.E. Amidon, G.L. Amidon, The biopharmaceutics classification system: subclasses for in vivo predictive dissolution (IPD) methodology and IVIVC, Eur. J. Pharm. Sci. 57 (2014) 152–163.
[13] C.A.S. Bergström, S.B. Andersson, J.H. Fagerberg, G. Ragnarsson, A. Lindahl, Is the full potential of the biopharmaceutics classification system reached? Eur. J. Pharm. Sci. 57 (2014) 224–231.
[14] J.H. Fagerberg, C.A.S. Bergström, Intestinal solubility and absorption of poorly water soluble compounds: predictions, challenges and solutions, Ther. Deliv. 6 (2015) 935–959.
[15] J.M. Butler, J.B. Dressman, The developability classification system: application of biopharmaceutics concepts to formulation development, J. Pharm. Sci. 99 (2010) 4940–4954.
[16] J. Rosenberger, J. Butler, J. Dressman, A refined developability classification system, J. Pharm. Sci. 107 (2018) 2020–2032.
[17] A. Fuchs, M. Leigh, B. Kloefer, J.B. Dressman, Advances in the design of fasted state simulating intestinal fluids: FaSSIF-V3, Eur. J. Pharm. Biopharm. 94 (2015) 229–240.
[18] J. Perrier, Z. Zhou, C. Dunn, I. Khadra, C.G. Wilson, G. Halbert, Statistical investigation of the full concentration range of fasted and fed simulated intestinal fluid on the equilibrium solubility of oral drugs, Eur. J. Pharm. Sci. 111 (2018) 247–256.
[19] B.E. Ainousah, J. Perrier, C. Dunn, I. Khadra, C.G. Wilson, G. Halbert, Dual level statistical investigation of equilibrium solubility in simulated fasted and fed intestinal fluid, Mol. Pharm. 14 (2017) 4170–4180.
[20] E. Galia, E. Nicolaides, D. Horter, R. Lobenberg, C. Reppas, J.B. Dressman, Evaluation of various dissolution media for predicting in vivo performance of class I and II drugs, Pharm. Res. 15 (1998) 698–705.
[21] E. Jantratid, N. Janssen, C. Reppas, J.B. Dressman, Dissolution media simulating conditions in the proximal human gastrointestinal tract: an update, Pharm. Res. 25 (2008) 1663–1676.
[22] A.A. Noyes, W.R. Whitney, The rate of solution of solid substances in their own solutions, J. Am. Chem. Soc. 19 (1897) 930–934.
[23] H.D. Williams, N.L. Trevaskis, S.A. Charman, R.M. Shanker, W.N. Charman, C.W. Pouton, C.J. Porter, Strategies to address low drug solubility in discovery and development, Pharmacol. Rev. 65 (2013) 315–499.
[24] J. Jinno, D.M. Oh, J.R. Crison, G.L. Amidon, Dissolution of ionizable water-insoluble drugs: The combined effect of pH and surfactant, J. Pharm. Sci. 89 (2000) 268–274.
[25] A. Balakrishnan, B.D. Rege, G.L. Amidon, J.E. Polli, Surfactant-mediated dissolution: contributions of solubility enhancement and relatively low micelle diffusivity, J. Pharm. Sci. 93 (2004) 2064–2075.
[26] W. Hayduk, H. Laudie, Prediction of diffusion coefficients for nonelectrolytes in dilute aqueous solutions, AIChE J. 20 (1974) 611–615.
[27] C.R. Wilke, P. Chang, Correlation of diffusion coefficients in dilute solutions, AIChE J. 1 (1955) 264–270.
[28] E.G. Scheibel, Physical chemistry in chemical engineering design, Ind. Eng. Chem. 46 (1954) 2007–2008.
[29] M.A. Lusis, C.A. Ratcliff, Diffusion in binary liquid mixtures at infinite dilution, Can. J. Chem. Eng. 46 (1968) 385–387.
[30] P. Stilbs, Fourier transform pulsed-gradient spin-echo studies of molecular diffusion, Prog. Nucl. Magn. Reson. Spectrosc. 19 (1987) 1–45.
[31] F. Ye, H. Jensen, S.W. Larsen, A. Yaghmur, C. Larsen, J. Østergaard, Measurement of drug diffusivities in pharmaceutical solvents using Taylor dispersion analysis, J. Pharm. Biomed. Anal. 61 (2012) 176–183.
[32] M.S. Bello, R. Rezzonico, P.G. Righetti, Use of taylor-aris dispersion for measurement of a solute diffusion coefficient in thin capillaries, Science 266 (1994) 773–776.
[33] A. Alizadeh, C.A. Nieto de Castro, W.A. Wakeham, The theory of the Taylor dispersion technique for liquid diffusivity measurements, Int. J. Thermophys. 1 (1980) 243–284.
[34] J.B. Dressman, G.L. Amidon, C. Reppas, V.P. Shah, Dissolution testing as a prognostic tool for oral drug absorption: immediate release dosage forms, Pharm. Res. 15 (1998) 11–22.
[35] Dissolution testing and acceptance criteria for immediate-release solid oral dosage form drug products containing high solubility drug substances. Guide for industry, U.S. Department of Health and Human Services, Food and Drug Administration, Center for Drug Evaluation and Research (CDER), 2018.
[36] J.H. Wood, J.E. Syarto, H. Letterman, Improved holder for intrinsic dissolution rate studies, J. Pharm. Sci. 54 (1965) 1068.
[37] A. Avdeef, O. Tsinman, Miniaturized rotating disk intrinsic dissolution rate measurement: effects of buffer capacity in comparisons to traditional Wood's apparatus, Pharm. Res. 25 (2008) 2613–2627.
[38] S.B.E. Andersson, C. Alvebratt, J. Bevernage, D. Bonneau, C. da Costa Mathews, R. Dattani, K. Edueng, Y. He, R. Holm, C. Madsen, T. Müller, U. Muenster, A. Müllertz, K. Ojala, T. Rades, P. Sieger, C.A.S. Bergström, Interlaboratory validation of small-scale solubility and dissolution measurements of poorly water-soluble drugs, J. Pharm. Sci. 105 (2016) 2864–2872.
[39] S.B.E. Andersson, C. Alvebratt, C.A.S. Bergström, Controlled suspensions enable rapid determinations of intrinsic dissolution rate and apparent solubility of poorly water-soluble compounds, Pharm. Res. 34 (2017) 1805–1816.
[40] K. Tsinman, A. Avdeef, O. Tsinman, D. Voloboy, Powder dissolution method for estimating rotating disk intrinsic dissolution rates of low solubility drugs, Pharm. Res. 26 (2009) 2093–2100.
[41] J. Plum, C.M. Madsen, A. Teleki, J. Bevernage, C. da Costa Mathews, E.M. Karlsson, S. Carlert, R. Holm, T. Müller, W. Matthews, A. Sayers, K. Ojala, K. Tsinsman, R. Lingamaneni, C.A.S. Bergström, T. Rades, A. Müllertz, Investigation of the intra- and interlaboratory reproducibility of a small scale standardized supersaturation and precipitation method, Mol. Pharm. 14 (2017)

4161–4169.
[42] K.J. Box, J. Comer, R. Taylor, S. Karki, R. Ruiz, R. Price, N. Fotaki, Small-scale assays for studying dissolution of pharmaceutical cocrystals for oral administration, AAPS Pharm. Sci. Tech. 17 (2016) 245–251.
[43] A. Ward, K. Walton, K. Box, J. Ostergaard, L.J. Gillie, B.R. Conway, K. Asare-Addo, Variable-focus microscopy and UV surface dissolution imaging as complementary techniques in intrinsic dissolution rate determination, Int. J. Pharm. 530 (2017) 139–144.
[44] J. Aaltonen, P. Heinänen, L. Peltonen, H. Kortejärvi, V.P. Tanninen, L. Christiansen, J. Hirvonen, J. Yliruusi, J. Rantanen, In situ measurement of solvent-mediated phase transformations during dissolution testing, J. Pharm. Sci. 95 (2006) 2730–2737.
[45] P.T. Mah, T. Laaksonen, T. Rades, J. Aaltonen, L. Peltonen, C.J. Strachan, Unravelling the relationship between degree of disorder and the dissolution behavior of milled glibenclamide, Mol. Pharm. 11 (2014) 234–242.
[46] L.X. Yu, A.S. Carlin, G.L. Amidon, A.S. Hussain, Feasibility studies of utilizing disk intrinsic dissolution rate to classify drugs, Int. J. Pharm. 270 (2004) 221–227.
[47] K.G. Mooney, M.A. Mintun, K.J. Himmelstein, V.J. Stella, Dissolution kinetics of carboxylic acids I: effect of pH under unbuffered conditions, J. Pharm. Sci. 70 (1981) 13–22.
[48] S. Li, S. Wong, S. Sethia, H. Almoazen, Y.M. Joshi, A.T.M. Serajuddin, Investigation of solubility and dissolution of a free base and two different salt forms as a function of pH, Pharm. Res. 22 (2005) 628–635.
[49] R.N. Jashnani, P.R. Byron, R.N. Dalby, Validation of an improved Wood's rotating disk dissolution apparatus, J. Pharm. Sci. 82 (1993) 670–671.
[50] R.N. Jashnani, R.N. Dalby, P.R. Byron, Preparation, characterization, and dissolution kinetics of two novel albuterol salts, J. Pharm. Sci. 82 (1993) 613–616.
[51] V.G. Levich, Physicochemical hydrodynamics, Prentice Hall, Englewood Cliffs, NJ, 1962.
[52] K.E. Johansson, J. Plum, M. Mosleh, C.M. Madsen, T. Rades, A. Mullertz, Characterization of the hydrodynamics in a miniaturized dissolution apparatus, J. Pharm. Sci. 107 (2018) 1095–1103.
[53] C.M. Berger, O. Tsinman, D. Voloboy, D. Lipp, S. Stones, A. Avdeef, Technical note: miniaturized intrinsic dissolution rate (Mini-IDR (TM)) measurement of griseofulvin and carbamazepine, Dissolut. Technol. 14 (2007) 39–41.
[54] Y.C. Tseng, M. Patel, Y.N. Zhao, Determination of intrinsic dissolution rate using miniaturized rotating and stationary disk systems, Dissolut. Technol. 21 (2014) 24–29.
[55] S. Klein, V.P. Shah, A standardized mini paddle apparatus as an alternative to the standard paddle, AAPS Pharm. Sci. Tech. 9 (2008) 1179–1184.
[56] E. Scheubel, M. Lindenberg, E. Beyssac, J.-M. Cardot, Small volume dissolution testing as a powerful method during pharmaceutical development, Pharmaceutics 2 (2010) 351.
[57] J. Alsenz, E. Haenel, A. Anedda, P. Du Castel, G. Cirelli, Miniaturized INtrinsic DISsolution Screening (MINDISS) assay for preformulation, Eur. J. Pharm. Sci. 87 (2016) 3–13.
[58] K. Greco, T.L. Bergman, R. Bogner, Design and characterization of a laminar flow-through dissolution apparatus: comparison of hydrodynamic conditions to those of common dissolution techniques, Pharm. Dev. Technol. 16 (2011) 75–87.
[59] K.G. Nelson, A.C. Shah, Convective diffusion-model for a transport-controlled dissolution rate process, J. Pharm. Sci. 64 (1975) 610–614.
[60] A.C. Shah, K.G. Nelson, Evaluation of a convective diffusion drug dissolution rate model, J. Pharm. Sci. 64 (1975) 1518–1520.
[61] K. Greco, D.P. McNamara, R. Bogner, Solution-mediated phase transformation of salts during dissolution: investigation using haloperidol as a model drug, J. Pharm. Sci. 100 (2011) 2755–2768.
[62] C.A.S. Bergström, R. Holm, S.A. Jørgensen, S.B.E. Andersson, P. Artursson, S. Beato, A. Borde, K. Box, M. Brewster, J. Dressman, K.-I. Feng, G. Halbert, E. Kostewicz, M. McAllister, U. Muenster, J. Thinnes, R. Taylor, A. Mullertz, Early pharmaceutical profiling to predict oral drug absorption: current status and unmet needs, Eur. J. Pharm. Sci. 57 (2014) 173–199.
[63] T. Young, III. An essay on the cohesion of fluids, Phil. Trans. R. Soc. Lond. 95 (1805) 65–87.
[64] M. Lazghab, K. Saleh, I. Pezron, P. Guigon, L. Komunjer, Wettability assessment of finely divided solids, Powder Technol. 157 (2005) 79–91.
[65] R. Holm, S. Borkenfelt, M. Allesø, J.E.T. Andersen, S. Beato, P. Holm, Investigation of surface porosity measurements and compaction pressure as means to ensure consistent contact angle determinations, Int. J. Pharm. 498 (2016) 355–361.
[66] M. Allesø, P. Holm, J.M. Carstensen, R. Holm, Quantitative surface topography assessment of directly compressed and roller compacted tablet cores using photometric stereo image analysis, Eur. J. Pharm. Sci. 87 (2016) 79–87.
[67] S.R. Modi, A.K.R. Dantuluri, S.R. Perumalla, C.Q.C. Sun, A.K. Bansal, Effect of crystal habit on intrinsic dissolution behavior of celecoxib due to differential wettability, Cryst. Growth Des. 14 (2014) 5283–5292.
[68] J.Y.Y. Heng, D.R. Williams, Wettability of paracetamol polymorphic forms I and II, Langmuir 22 (2006) 6905–6909.
[69] J.Y.Y. Heng, A. Bismarck, D.R. Williams, Anisotropic surface chemistry of crystalline pharmaceutical solids, AAPS Pharm. Sci. Tech. 7 (2006) E12–E20.
[70] A. Niederquell, M. Kuentz, Biorelevant dissolution of poorly soluble weak acids studied by UV imaging reveals ranges of fractal-like kinetics, Int. J. Pharm. 463 (2014) 38–49.
[71] N. Qiao, K. Wang, W. Schlindwein, A. Davies, M. Li, In situ monitoring of carbamazepine–nicotinamide cocrystal intrinsic dissolution behaviour, Eur. J. Pharm. Biopharm. 83 (2013) 415–426.
[72] J.X. Wu, S. Rehder, F.v.d. Berg, J.M. Amigo, J.M. Carstensen, T. Rades, C.S. Leopold, J. Rantanen, Chemical imaging and solid state analysis at compact surfaces using UV imaging, Int. J. Pharm. 477 (2014) 527–535.
[73] A. Avdeef, K. Tsinman, O. Tsinman, N. Sun, D. Voloboy, Miniaturization of powder dissolution measurement and estimation of particle size, Chem. Biodivers. 6 (2009) 1796–1811.
[74] A. Dokoumetzidis, P. Macheras, A century of dissolution research: from Noyes and Whitney to the biopharmaceutics classification system, Int. J. Pharm. 321 (2006) 1–11.
[75] A.P. Tinke, K. Vanhoutte, R. De Maesschalck, S. Verheyen, H. De Winter, A new approach in the prediction of the dissolution behavior of suspended particles by means of their particle size distribution, J. Pharm. Biomed. Anal. 39 (2005) 900–907.
[76] M. Mosharraf, C. Nyström, The effect of particle size and shape on the surface specific dissolution rate of microsized practically insoluble drugs, Int. J. Pharm. 122 (1995) 35–47.
[77] C. Nyström, M. Westerberg, The use of ordered mixtures for improving the dissolution rate of low solubility compounds, J. Pharm. Pharmacol. 38 (1986) 161–165.
[78] B. Zuo, Y. Sun, H. Li, X. Liu, Y. Zhai, J. Sun, Z. He, Preparation and in vitro/in vivo evaluation of fenofibrate nanocrystals, Int. J. Pharm. 455 (2013) 267–275.
[79] A. Bitterlich, C. Laabs, I. Krautstrunk, M. Dengler, M. Juhnke, A. Grandeury, H. Bunjes, A. Kwade, Process parameter dependent growth phenomena of naproxen nanosuspension manufactured by wet media milling, Eur. J. Pharm. Biopharm. 92 (2015) 171–179.
[80] L. Lindfors, P. Skantze, U. Skantze, J. Westergren, U. Olsson, Amorphous drug nanosuspensions. 3. Particle dissolution and crystal growth, Langmuir 23 (2007) 9866–9874.
[81] I.-H. Baek, J.-S. Kim, E.-S. Ha, G.-H. Choo, W. Cho, S.-J. Hwang, M.-S. Kim, Dissolution and oral absorption of pranlukast nanosuspensions stabilized by hydroxypropylmethyl cellulose, Int. J. Biol. Macromol. 67 (2014) 53–57.
[82] C.M. Keck, R.H. Muller, Drug nanocrystals of poorly soluble drugs produced by high pressure homogenisation, Eur. J. Pharm. Biopharm. 62 (2006) 3–16.
[83] E. Merisko-Liversidge, G.G. Liversidge, E.R. Cooper, Nanosizing: a formulation approach for poorly-water-soluble compounds, Eur. J. Pharm. Sci. 18 (2003) 113–120.
[84] L. Wu, J. Zhang, W. Watanabe, Physical and chemical stability of drug nanoparticles, Adv. Drug Deliv. Rev. 63 (2011) 456–469.
[85] B. Van Eerdenbrugh, J. Vermant, J.A. Martens, L. Froyen, J. Van Humbeeck, P. Augustijns, G. Van Den Mooter, A screening study of surface stabilization during the production of drug nanocrystals, J. Pharm. Sci. 98 (2009) 2091–2103.
[86] A.M. Cerdeira, M. Mazzotti, B. Gander, Formulation and drying of miconazole and itraconazole nanosuspensions, Int. J. Pharm. 443 (2013) 209–220.
[87] B. Shekunov, E.R. Montgomery, Theoretical analysis of drug dissolution: I. Solubility and intrinsic dissolution rate, J. Pharm. Sci. 105 (2016) 2685–2697.
[88] N. Li, M.D. DeGennar, W. Liebenberg, L.R. Tiedt, A.S. Zahn, M.V. Pishko, M.M. de Villiers, Increased dissolution and physical stability of micronized nifedipine particles encapsulated with a biocompatible polymer and surfactants in a wet ball milling process, Pharmazie 61 (2006) 595–603.
[89] M. Kuentz, Analytical technologies for real-time drug dissolution and precipitation testing on a small scale, J. Pharm. Pharmacol. 67 (2015) 143–159.
[90] A. Paudel, D. Raijada, J. Rantanen, Raman spectroscopy in pharmaceutical product design, Adv. Drug Deliv. Rev. 89 (2015) 3–20.
[91] C. Stillhart, G. Imanidis, M. Kuentz, Insights into drug precipitation kinetics during in vitro digestion of a lipid-based drug delivery system using in-line Raman spectroscopy and mathematical modeling, Pharm. Res. 30 (2013) 3114–3130.
[92] Y. Kuroiwa, K. Higashi, K. Ueda, K. Yamamoto, K. Moribe, Nano-scale and molecular-level understanding of wet-milled indomethacin/poloxamer 407 nanosuspension with TEM, suspended-state NMR, and Raman measurements, Int. J. Pharm. 537 (2018) 30–39.
[93] Y.X. Wang, B. Abrahamsson, L. Lindfors, J.G. Brasseur, Analysis of diffusion-controlled dissolution from polydisperse collections of drug particles with an assessed mathematical model, J. Pharm. Sci. 104 (2015) 2998–3017.
[94] G. Shiko, L.F. Gladden, A.J. Sederman, P.C. Connolly, J.M. Butler, MRI studies of the hydrodynamics in a USP 4 dissolution testing cell, J. Pharm. Sci. 100 (2011) 976–991.
[95] B. Wang, G. Bredael, P.M. Armenante, Computational hydrodynamic comparison of a mini vessel and a USP 2 dissolution testing system to predict the dynamic operating conditions for similarity of dissolution performance, Int. J. Pharm. 539 (2018) 112–130.
[96] S. Neervannan, M.Z. Southard, V.J. Stella, Dissolution of weak acids under laminar flow and rotating disk hydrodynamic conditions: application of a comprehensive convection-diffusion-migration-reaction transport model, J. Pharm. Sci. 101 (2012) 3180–3189.
[97] L. Lindfors, M. Jonsson, E. Weibull, J.G. Brasseur, B. Abrahamsson, Hydrodynamic effects on drug dissolution and deaggregation in the small intestine – a study with felodipine as a model drug, J. Pharm. Sci. 104 (2015) 2969–2976.
[98] P. Lehto, J. Aaltonen, M. Tenho, J. Rantanen, J. Hirvonen, V.P. Tanninen, L. Peltonen, Solvent-mediated solid phase transformations of carbamazepine: effects of simulated intestinal fluid and fasted state simulated intestinal fluid, J. Pharm. Sci. 98 (2009) 985–996.
[99] J.H. Fagerberg, Y. Al-Tikriti, G. Ragnarsson, C.A.S. Bergström, Ethanol effects on apparent solubility of poorly soluble drugs in simulated intestinal fluid, Mol. Pharm. 9 (2012) 1942–1952.
[100] L.H. Nielsen, J. Nagstrup, S. Gordon, S.S. Keller, J. Ostergaard, T. Rades, A. Mullertz, A. Boisen, pH-triggered drug release from biodegradable microwells for oral drug delivery, Biomed. Microdevices 17 (2015) 9958.
[101] H. Palmelund, C.M. Madsen, J. Plum, A. Mullertz, T. Rades, Studying the

propensity of compounds to supersaturate: a practical and broadly applicable approach, J. Pharm. Sci. 105 (2016) 3021–3029.
[102] E. Borbas, Z.K. Nagy, B. Nagy, A. Balogh, B. Farkas, O. Tsinman, K. Tsinman, B. Sinko, The effect of formulation additives on in vitro dissolution-absorption profile and in vivo bioavailability of telmisartan from brand and generic formulations, Eur. J. Pharm. Sci. 114 (2018) 310–317.
[103] E. Borbas, P. Tozser, K. Tsinman, O. Tsinman, K. Takacs-Novak, G. Volgyi, B. Sinko, Z.K. Nagy, Effect of formulation additives on drug transport through size-exclusion membranes, Mol. Pharm. 15 (2018) 3308–3317.
[104] C. Alvebratt, O. Cheung, M. Stromme, C.A.S. Bergström, A modified in situ method to determine release from a complex drug carrier in particle-rich suspensions, AAPS Pharm. Sci. Tech. (2018).
[105] T. Gravestock, K. Box, J. Comer, E. Frake, S. Judge, R. Ruiz, The “GI dissolution” method: a low volume, in vitro apparatus for assessing the dissolution/precipitation behaviour of an active pharmaceutical ingredient under biorelevant conditions, Anal. Methods 3 (2011) 560–567.
[106] P.J. O'Dwyer, C. Litou, K.J. Box, J.B. Dressman, E.S. Kostewicz, M. Kuentz, C. Reppas, In vitro methods to assess drug precipitation in the fasted small intestine – a PEARRL review, J. Pharm Pharmacol (2018).
[107] J. Ostergaard, UV imaging in pharmaceutical analysis, J. Pharm. Biomed. Anal. 147 (2018) 140–148.
[108] S.S. Jensen, H. Jensen, D.M. Goodall, J. Ostergaard, Performance characteristics of UV imaging instrumentation for diffusion, dissolution and release testing studies, J. Pharm. Biomed. Anal. 131 (2016) 113–123.
[109] S. Gordon, K. Naelapaa, J. Rantanen, A. Selen, A. Mullertz, J. Ostergaard, Real-time dissolution behavior of furosemide in biorelevant media as determined by UV imaging, Pharm. Dev. Technol. 18 (2013) 1407–1416.
[110] L.H. Nielsen, S. Gordon, J.P. Pajander, J. Østergaard, T. Rades, A. Müllertz, Biorelevant characterisation of amorphous furosemide salt exhibits conversion to a furosemide hydrate during dissolution, Int. J. Pharm. 457 (2013) 14–24.
[111] J. Østergaard, J.X. Wu, K. Naelapää, J.P. Boetker, H. Jensen, J. Rantanen, Simultaneous UV imaging and Raman spectroscopy for the measurement of solvent-mediated phase transformations during dissolution testing, J. Pharm. Sci. 103 (2014) 1149–1156.
[112] S. Colombo, M. Brisander, J. Haglöf, P. Sjövall, P. Andersson, J. Østergaard, M. Malmsten, Matrix effects in nilotinib formulations with pH-responsive polymer produced by carbon dioxide-mediated precipitation, Int. J. Pharm. 494 (2015) 205–217.
[113] J.P. Boetker, M. Savolainen, V. Koradia, F. Tian, T. Rades, A. Mullertz, C. Cornett, J. Rantanen, J. Ostergaard, Insights into the early dissolution events of amlodipine using UV imaging and Raman spectroscopy, Mol. Pharm. 8 (2011) 1372–1380.
[114] S. Svanback, H. Ehlers, O. Antikainen, J. Yliruusi, High-speed intrinsic dissolution rate in one minute using the single-particle intrinsic dissolution rate method, Anal. Chem. 87 (2015) 11058–11064.
[115] S. Svanback, H. Ehlers, J. Yliruusi, Optical microscopy as a comparative analytical technique for single-particle dissolution studies, Int. J. Pharm. 469 (2014) 10–16.
[116] S. Svanback, H. Ehlers, O. Antikainen, J. Yliruusi, On-chip optofluidic single-particle method for rapid microscale equilibrium solubility screening of biologically active substances, Anal. Chem. 87 (2015) 5041–5045.
[117] K.V. Prasad, R.I. Ristic, D.B. Sheen, J.N. Sherwood, Dissolution kinetics of paracetamol single crystals, Int. J. Pharm. 238 (2002) 29–41.
[118] S.L. Raghavan, R.I. Ristic, D.B. Sheen, J.N. Sherwood, Dissolution kinetics of single crystals of alpha-lactose monohydrate, J. Pharm. Sci. 91 (2002) 2166–2174.
[119] A.C. Hillier, M.D. Ward, Atomic force microscopy of the electrochemical nucleation and growth of molecular crystals, Science 263 (1994) 1261–1264.
[120] T.R. Keel, C. Thompson, M.C. Davies, S.J. Tendler, C.J. Roberts, AFM studies of the crystallization and habit modification of an excipient material, adipic acid, Int. J. Pharm. 280 (2004) 185–198.
[121] M. Valtiner, S. Borodin, G. Grundmeier, Stabilization and acidic dissolution mechanism of single-crystalline ZnO(0001) surfaces in electrolytes studied by in-situ AFM imaging and ex-situ LEED, Langmuir 24 (2008) 5350–5358.
[122] D.P. Burt, N.R. Wilson, U. Janus, J.V. Macpherson, P.R. Unwin, In-situ atomic force microscopy (AFM) imaging: influence of AFM probe geometry on diffusion to microscopic surfaces, Langmuir 24 (2008) 12867–12876.
[123] J. Ostergaard, F. Ye, J. Rantanen, A. Yaghmur, S.W. Larsen, C. Larsen, H. Jensen, Monitoring lidocaine single-crystal dissolution by ultraviolet imaging, J. Pharm. Sci. 100 (2011) 3405–3410.
[124] J.N. Clark, J. Ihli, A.S. Schenk, Y.Y. Kim, A.N. Kulak, J.M. Campbell, G. Nisbet, F.C. Meldrum, I.K. Robinson, Three-dimensional imaging of dislocation propagation during crystal growth and dissolution, Nat. Mater. 14 (2015) 780–784.
[125] K. Wlodarski, W. Sawicki, K. Haber, J. Knapik, Z. Wojnarowska, M. Paluch, P. Lepek, L. Hawelek, L. Tajber, Physicochemical properties of tadalafil solid dispersions – impact of polymer on the apparent solubility and dissolution rate of tadalafil, Eur. J. Pharm. Biopharm. 94 (2015) 106–115.
[126] V. Bhardwaj, N.S. Trasi, D.Y. Zemlyanov, L.S. Taylor, Surface area normalized dissolution to study differences in itraconazole-copovidone solid dispersions prepared by spray-drying and hot melt extrusion, Int. J. Pharm. 540 (2018) 106–119.
[127] F. Sami, B. Philip, K. Pathak, Effect of auxiliary substances on complexation efficiency and intrinsic dissolution rate of gemfibrozil-beta-CD complexes, AAPS Pharm. Sci. Tech. 11 (2010) 27–35.
[128] Y. Lu, M. Li, Simultaneous rapid determination of the solubility and diffusion coefficients of a poorly water-soluble drug based on a novel UV imaging system, J. Pharm. Sci. 105 (2016) 131–138.
[129] E.S. Kostewicz, B. Abrahamsson, M. Brewster, J. Brouwers, J. Butler, S. Carlert, P.A. Dickinson, J. Dressman, R. Holm, S. Klein, J. Mann, M. McAllister, M. Minekus, U. Muenster, A. Mullertz, M. Verwei, M. Vertzoni, W. Weitschies, P. Augustijns, In vitro models for the prediction of in vivo performance of oral dosage forms, Eur. J. Pharm. Sci. 57 (2014) 342–366.
[130] P. Zakeri-Milani, M. Barzegar-Jalali, M. Azimi, H. Valizadeh, Biopharmaceutical classification of drugs using intrinsic dissolution rate (IDR) and rat intestinal permeability, Eur. J. Pharm. Biopharm. 73 (2009) 102–106.
[131] U. Muenster, W. Mueck, D. van der Mey, K.H. Schlemmer, S. Greschat-Schade, M. Haerter, C. Pelzetter, C. Pruemper, J. Verlage, A.H. Goller, A. Ohm, Predicting biopharmaceutical performance of oral drug candidates – extending the volume to dissolve applied dose concept, Eur. J. Pharm. Biopharm. 102 (2016) 191–201.
[132] U. Muenster, C. Pelzetter, T. Backensfeld, A. Ohm, T. Kuhlmann, H. Mueller, K. Lustig, J. Keldenich, S. Greschat, A.H. Goller, M.J. Gnoth, Volume to dissolve applied dose (VDAD) and apparent dissolution rate (ADR): tools to predict in vivo bioavailability from orally applied drug suspensions, Eur. J. Pharm. Biopharm. 78 (2011) 522–530.
[133] J. Zhang, D. Liu, Y. Huang, Y. Gao, S. Qian, Biopharmaceutics classification and intestinal absorption study of apigenin, Int. J. Pharm. 436 (2012) 311–317.